

Theory of magnetotransport in two-dimensional electron systems subjected to weak two-dimensional superlattice potentials

Daniela Pfannkuche and Rolf R. Gerhardt

Max-Planck-Institut für Festkörperforschung, Heisenbergstrasse 1, D-7000 Stuttgart 80, Federal Republic of Germany

(Received 6 July 92)

The recently observed resistance oscillations of a two-dimensional (2D) electron system subject to a weak lateral 2D superlattice potential and a perpendicular magnetic field are investigated theoretically. Generalizing previous work on 1D superlattices, we develop a magnetotransport theory based on a quantum-mechanical picture taking consistently into account the effect of the lateral superlattice on the energy spectrum and the effect of randomly distributed impurities on collision broadening and transport scattering rate. The superlattice lifts the degeneracy of the Landau levels and leads to Landau bands with an oscillatory width and a complicated internal subband structure, visualized by the famous self-similar "Hofstadter butterfly." The interplay between this peculiar energy spectrum and collision broadening effects is shown to provide the key for the understanding of all the characteristic features of the magnetotransport oscillations reported in recent experimental work.

I. INTRODUCTION

In recent years magnetotransport properties of two-dimensional electron systems (2D ES's) with lateral superlattices have attracted increasing interest. In addition to the Shubnikov-de Haas (SdH) oscillations, which are known from homogeneous 2D ES's in a perpendicular quantizing magnetic field B , the periodically modulated 2D ES's exhibit characteristic oscillations at low B values. The nature of these oscillations depends on the type of superlattice imposed on the 2D ES.

In their pioneering experiments, Weiss *et al.*¹ investigated 2D ES's in $\text{Al}_x\text{Ga}_{1-x}\text{As-GaAs}$ heterostructures with a weak 1D superlattice potential. The lateral superlattice was produced by means of an ingenious holographic technique exploiting the persistent photoconductivity effect in Si-doped $\text{Al}_x\text{Ga}_{1-x}\text{As}$ at low temperatures. The resulting high-mobility samples ($\mu > 10^6$ cm^2/Vs , mean free path $\lambda_{\text{free}} > 10$ μm , modulation period $a \sim 300$ nm) showed well-resolved and strongly anisotropic magnetoresistance oscillations at low magnetic fields, which were distinctly different from the SdH oscillations appearing at higher B values.

Similar to the SdH oscillations, the modulation-induced oscillations ("Weiss oscillations") are periodic in B^{-1} . Extrema occur at B values, for which the cyclotron radius $R_c = l^2 k_F = v_F/\omega_c$ of electrons at the Fermi energy $E_F = \hbar^2 k_F^2/2m$ becomes commensurate with the superlattice period a ,

$$2R_c = a(\lambda - \frac{1}{4}), \quad \lambda = 1, 2, \dots \quad (1)$$

Here $l = (c\hbar/eB)^{1/2}$ is the magnetic length, $\omega_c = eB/mc$ the cyclotron frequency, $v_F = \hbar k_F/m$ the Fermi velocity, and $m = 0.067m_0$ the effective mass of GaAs. From a microscopic point of view, this condition involves three fundamental characteristic lengths of the 2D ES, namely

the period a , the magnetic length l , and the Fermi wavelength $\lambda_F = 2\pi/k_F$, which depends on the area density $N_s = k_F^2/2\pi$ ($\sim 3 \times 10^{11}$ cm^{-2}) of the 2D ES. The minima of the SdH oscillations, on the other hand, occur at integer values of the filling factor $\nu = 2\pi l^2 N_s$ of the Landau levels, so that the SdH period in B^{-1} is determined only by the two lengths l and λ_F .

The Weiss oscillations introduced by weak 1D superlattice potentials have been investigated theoretically by several authors²⁻⁹ and are now well understood. Certain aspects of the phenomenon can be explained within a quasiclassical picture. Especially the large-amplitude magnetoresistance oscillations, observed when the current flows perpendicular to the equipotentials, are attributed to the guiding-center drift of cyclotron orbits in the weak periodic electric field created by the superlattice.^{5,10-12} An alternative semiclassical approach,⁹ emphasizing the importance of magnetic breakdown effects, is also able to explain these large-amplitude oscillations and, moreover, the strong positive magnetoresistance at very low magnetic fields, which has always been observed together with these oscillations. In the present paper we will not consider this low-field regime, and rather concentrate on the oscillatory effects at higher magnetic fields. For a full understanding of the Weiss oscillations observed on the different components of the resistance tensor, a quantum transport theory is necessary.^{7,8} The key feature is that the superlattice potential lifts the degeneracy of the Landau levels (LL's) and leads to Landau bands of oscillating width. This bandwidth becomes minimum for the n th LL, if the condition (1) is satisfied for the cyclotron radius corresponding to this LL, $R_c = R_n \equiv l\sqrt{2n+1}$. This minimum bandwidth is accompanied by a maximum height of the density-of-states (DOS) peak contributed by this LL ("partial DOS" of this LL). The amplitude oscillation of

the Landau DOS related to this bandwidth oscillation has been observed directly in the magnetocapacitance.^{13,14} Another direct proof of the quantum origin of the phenomenon is the fact that at lower temperatures the Weiss oscillations occur as an amplitude modulation of the SdH oscillations.^{15,16} As further consequences of these bandwidth oscillations, Weiss-type oscillations have been predicted for the thermomagnetic transport coefficients¹⁷ and for collective excitations.¹⁸ The Weiss oscillations have also been observed in magnetoresistance experiments on samples with microstructured gates, where the 1D modulation strength could be tuned by the gate voltage.^{3,10} If the modulation amplitude becomes too large, the Weiss oscillations disappear.¹⁰

Recently, also the effect of two-dimensional superlattices on the magnetotransport properties of 2D ES's have been studied experimentally, both in the limit of a weak modulation^{15,16,19–22} and for a very strong modulation, where forbidden “antidot” regions are punched through the 2D ES.^{23,24} From the theoretical point of view this is a very interesting situation: The two-dimensional motion of the electrons in the presence of both a 2D superlattice of period a [$a = (a_x a_y)^{1/2}$ for a rectangular symmetry with periods a_x and a_y] and a perpendicular magnetic field B leads to intricate commensurability problems due to the interplay of the two length scales a and l . The single-particle spectrum for this situation has been investigated theoretically by many authors for more than three decades.^{25–31} For a simple cosine-potential on a superlattice with square symmetry, the energy spectrum as a function of B shows a complicated self-similar structure, visualized by the highly aesthetic graph known as Hofstadter's butterfly.²⁹ This result is obtained in the two complementary, but mathematically equivalent limits²⁷ of, first, a strong lattice potential and a weak magnetic field in the tight-binding approximation,^{25,27,29} and, second, a weak periodic perturbation of a Landau-quantized 2D ES.^{27,30,31} In both limiting cases, the energy spectrum can be calculated by elementary methods only if the magnetic flux per unit cell, $\Phi = Ba^2$, is a rational multiple of the flux quantum $\Phi_0 = hc/e$, i.e., if

$$\Phi/\Phi_0 \equiv a^2/2\pi l^2 = p/q, \quad (2)$$

with integers p and q which are relative prime. This is a commensurability condition for the lattice period a and the magnetic length l .

Historically, the tight-binding calculations, which include the magnetic field by means of the Peierls substitution, have been studied first. Aiming at the quantized Hall effect (QHE), later on also the conductivity tensor has been calculated in this spirit on the basis of a (small-size) lattice model including disorder within the coherent-potential approximation (CPA).³² Such calculations are applicable to situations where the conduction band at the Fermi energy is energetically well separated from all other bands. This may be the case for bands owing to the strong periodic modulation by a natural (atomic) crystal potential ($a \sim 0.5$ nm). The situation in the artificial superlattices studied so far is, however, quite different. For typical lattice constants ($a \sim 300$ nm) and

electron densities ($N_s \sim 3 \times 10^{11}$ cm⁻²), about 50 spin-degenerate bands ($\sim a^2 N_s/2$) are occupied, and several (overlapping) bands are located at or close to the Fermi energy. In this situation, a quasiclassical description of the electron motion seems more appropriate. Indeed, the (nonperiodic) magnetoresistance oscillations observed recently on “antidot” superlattices²⁴ have been explained in terms of commensurate classical orbits,^{24,33} and the importance of classical chaotic motion in this case has been emphasized.³³

Whereas the tight-binding calculations for strong modulation and weak magnetic field have, at present, no relevance to the 2D ES's in artificial superlattices, the situation is different for the opposite limit of a weak modulation and a strong magnetic field, which we will consider exclusively in the following. For systems without disorder, this limit has been discussed as a model for the QHE.^{34,35,30} In the present paper we will incorporate knowledge about the highly complex single-particle energy spectrum into a transport theory, which takes the effect of disorder on the broadening of the Landau levels and on the transport scattering rate into account in the spirit of the self-consistent Born approximation³⁶ for randomly distributed (short-range) scatterers. Our main purpose is to demonstrate in a comprehensible manner that this extension of previous work on 2D ES's with a weak 1D superlattice^{7,8} indeed is capable of explaining all the essential features of the Weiss oscillations observed on samples with a weak 2D superlattice potential.

The assumption of a weak superlattice potential is essential for our approach. It guarantees that, for the range of magnetic fields we are interested in, the lateral superlattice does not lead to a mixing of LL's, and that it can be treated in lowest-order perturbation expansion. Then, the most important effect of the 2D superlattice is to split each Landau band into subbands. For a simple cosine potential on a lattice with square symmetry, each Landau band splits into p subbands (which are q -fold degenerate) if Eq. (2) holds. The overall width of the modulation-broadened Landau bands, on the other hand, has the same oscillatory dependence on the LL index n and the magnetic field as for a 1D superlattice, with minima if Eq. (1) is satisfied. This is the reason why the magnetoresistance oscillations observed on samples with a 2D superlattice have the same period in B^{-1} as those with a 1D superlattice of the same lattice constant and with the same density. Experimentally, such a comparison between 1D and 2D modulation has been carried out most directly by a successive two-step holographic illumination (with rotation of the sample by 90° after the first step) of the same sample, keeping all other parameters fixed.^{15,20}

The theory to be presented here is also capable of explaining the striking differences between the Weiss oscillations observed on samples with a 1D and those with a 2D lateral superlattice, respectively. A sample with a 1D modulation in the x direction shows weak Weiss oscillations of $\rho_{yy}^{(1D)}$, the resistivity component measured when the current flows parallel to the equipotentials of the modulation, with maxima when Eq. (1) holds. For the correct explanation of these oscillations as quantum oscil-

lations of the scattering rate,⁸ a self-consistent treatment of scattering rate and collision broadening has turned out to be necessary, as we will emphasize in Sec. IV. The resistivity component $\rho_{xx}^{(1D)}$, measured when the current flows perpendicular to the equipotentials, shows Weiss oscillations with much larger amplitudes and a phase shift of π , so that $\rho_{xx}^{(1D)}$ has minima if Eq. (1) holds and $\rho_{yy}^{(1D)}$ has maxima. These large-amplitude oscillations are attributed to an additional conductance mechanism in the modulated samples, a “band conductivity,” related to the guiding-center drift of cyclotron orbits in the y direction.^{2,3,5,8} Experimentally, a dramatic reduction of the large-amplitude oscillations is observed after the second illumination step, i.e., after the modulation in the second lateral direction, and only the weaker antiphase oscillations related to the scattering-rate oscillations survive.

Such a dramatic suppression of the band conductivity follows from our theory for situations with such a small collision broadening that (at zero temperature) the modulation-induced subband splitting of the LL’s is partially resolved. Moreover, by changing the relative strength of collision broadening and 2D superlattice potential, we can switch between situations in which the band conductivity dominates the Weiss oscillations and those in which the oscillations of the scattering rate dominate, in agreement with recent experiments on gated samples.¹⁶ The suppression of the band conductivity is a genuine quantum effect and does not exist in a classical treatment.¹² An indication of this effect was found in the recent work of Štréda, Kučera, and van de Konijnenberg,³⁷ who incorporated only the periodic potential in one lateral direction into the energy spectrum. Using Fermi’s golden rule, they then calculated the probability of Bragg reflections due to the periodic potential in the other direction perturbatively. The band conductivity was related to this reflection probability, and it was found to be suppressed if the collision broadening becomes of the order of or smaller than the modulation-induced width of the Landau bands. Thus, this semiclassical approach³⁷ points towards the correct origin of the suppression of the band conductivity. A weak point of this approach, however, is that the 2D superlattice potential is treated differently in the two lateral directions, and, therefore, the energy spectrum is not taken into account in a consistent manner.

Several authors^{21,22,38,39} have previously appreciated the need for a transport theory which correctly includes the effect of the 2D superlattice potential on the single-particle energies. But attempts in this context were either restricted to the classical limit,²¹ or suffered from an unjustified truncation³⁸ of the correct generalization of Harper’s equation (see Sec. III) leading to unreliable results, or the magnetic field was restricted to special values^{39,40} for which the internal structure of the LL’s becomes trivial without subband splitting. A satisfactory theory of all the aspects of the Weiss oscillations, however, has not been developed before.

The organization of the paper is as follows. In order to make the paper essentially self-contained, we recall in

Sec. II the results on the single-particle spectrum which we will need in the following sections. These results are not new, but they are spread over the literature and it is, hopefully, helpful for the reader to find them collected under a unified perspective and with a unified notation. In Sec. III we adapt the treatment of collision broadening developed for 1D superlattices⁸ to the 2D case, and we calculate the DOS. In Sec. IV we derive and evaluate the corresponding approximation for the conductivity tensor. For the diagonal components, we discuss in detail the “band-conductivity” and the “scattering-conductivity” contributions. The Hall conductivity is discussed in light of previous work on systems without disorder,³⁰ emphasizing that the subband splitting of the Hofstadter-type spectrum leads to integer-quantized values. In Sec. V, finally, we present some numerical results, and we discuss the achievements and the limitations of our approach.

The numerical results presented here have been calculated for simple cosine potentials on a square lattice. This is sufficient for the present illustrative purpose. For a direct comparison with experiments, it might, however, be desirable to include higher harmonics. Therefore, we develop the analytical formulation of our transport theory for the more general case of a 2D superlattice potential with arbitrary Fourier coefficients on a rectangular lattice. Apart from possible future applications, we are thus able to give a microscopic justification of a recent calculation of the band conductivity for arbitrary rectangular superlattice potentials in the quasiclassical limit.¹² Some preliminary results and model calculations based on the present work have been published before²⁰ and quoted elsewhere.^{15,41} A coherent presentation of our approach in its general form is given here.

II. ENERGY SPECTRUM

A. Model

For typical samples showing the Weiss oscillations, the mean free path ($\sim 10 \mu\text{m}$) is much larger than the lattice constant ($\sim 100\text{--}300 \text{ nm}$) and, for $B \geq 0.1 \text{ T}$, even much larger than the cyclotron radius at the Fermi energy ($R_c \leq 0.9 \mu\text{m}$). Therefore, quantum interference effects due to the superlattice potential have to be taken into account, and will be included in our model.

We consider the single-electron Hamiltonian

$$H = \frac{1}{2m} \left[\mathbf{p} + \frac{e}{c} \mathbf{A}(\mathbf{r}) \right]^2 + V(\mathbf{r}), \quad (3)$$

where $-e$ is the charge of an electron and all the vectors are in the x - y plane. The potential has a Fourier expansion of the general form

$$V(\mathbf{r}) = \sum_{\mathbf{g}} V_{\mathbf{g}} e^{i\mathbf{g}\cdot\mathbf{r}}, \quad \mathbf{g} = (n_x K_x, n_y K_y) \quad (4)$$

on a rectangular superlattice, where n_x and n_y are integers, and $a_x = 2\pi/K_x$ and $a_y = 2\pi/K_y$ are the lattice constants. Explicit numerical results will be given for the simple special case

$$V(\mathbf{r}) = V_x \cos(K_x x) + V_y \cos(K_y y) + V_{xy} \cos(K_x x) \cos(K_y y), \quad (5)$$

i.e., for $2V_{(\pm K_x, 0)} = V_x$, $2V_{(0, \pm K_y)} = V_y$, $4V_{(\pm K_x, \pm K_y)} = V_{xy}$, and $V_{\mathbf{g}} = 0$ if $n_x^2 + n_y^2 > 2$.

The unmodulated [$V(\mathbf{r}) \equiv 0$] system has energy eigenvalues $E_n = \hbar\omega_c(n + \frac{1}{2})$ and, in the Landau gauge for the vector potential, $\mathbf{A}(\mathbf{r}) = (0, xB)$, one obtains the eigenstates $|n, k_y\rangle$ with wave functions⁴²

$$\psi_{nk_y}(x, y) = L_y^{-1/2} \exp(ik_y y) \phi_n(x - x_0), \quad (6)$$

where $x_0 = -l^2 k_y$, and ϕ_n is a normalized oscillator function. We calculate the effect of the modulation potential $V(\mathbf{r})$ by diagonalization of the Hamiltonian (3) in this set of basis functions. The matrix element of an arbitrary 2D-potential Fourier component follows from

$$\begin{aligned} & \langle n' k'_y | \exp(i\mathbf{q} \cdot \mathbf{r}) | n, k_y \rangle \\ &= \delta_{k'_y, k_y + q_y} \exp \left[-\frac{i}{2} l^2 q_x (k'_y + k_y) \right] \mathcal{L}_{n', n}(\mathbf{q}) \end{aligned} \quad (7)$$

with

$$\begin{aligned} \mathcal{L}_{n', n}(\mathbf{q}) &= (m!/M!)^{\frac{1}{2}} i^{|n'-n|} [(q_x + iq_y)/q]^{n-n'} \\ &\times e^{-\frac{1}{2}Q} Q^{\frac{1}{2}|n'-n|} L_m^{(|n'-n|)}(Q), \end{aligned} \quad (8)$$

where m and M are the minimum and the maximum of n' and n , respectively, $q = (q_x^2 + q_y^2)^{1/2}$, $Q = \frac{1}{2} l^2 q^2$, and $L_m^{(\alpha)}(Q)$ is an associated Laguerre polynomial. In the following, we will need mainly the intra-LL matrix elements with $n' = n$, which allow the simplification

$$\begin{aligned} \mathcal{L}_{n, n}(\mathbf{q}) &\equiv \mathcal{L}_n(Q) = \exp(-\frac{1}{2}Q) L_n(Q) \\ &\approx J_0(qR_n) \approx \left(\frac{2}{\pi q R_n} \right)^{1/2} \cos \left(qR_n - \frac{\pi}{4} \right), \end{aligned} \quad (9)$$

where we have indicated the asymptotic form for large n , with J_0 the Bessel function of order zero and $R_n = l\sqrt{2n+1}$ the cyclotron radius related to the n th LL.

B. Two-dimensional superlattice

1. Magnetic translations

With a modulation in the x direction only, k_y remains a good quantum number, and the eigenstates and energies can be classified by the quantum numbers n and x_0 .⁸ The modulation in the y direction destroys the translational invariance in this direction, and the matrix elements (7) are no longer diagonal with respect to k_y . Physically, this additional modulation leads to additional Bragg scattering, and thus to a subband splitting of the Landau bands owing to a 1D modulation.⁸ The relevant quantum numbers result from a simple consideration of the ‘‘magnetic translation group.’’^{43,31} Let us consider a rectangular superlattice with basis vectors $\mathbf{a} = (a_x, 0)$ and $\mathbf{b} = (0, a_y)$, so that the potential is invariant under the translations by $\mathbf{R} = n\mathbf{a} + m\mathbf{b}$, $V(\mathbf{r} + \mathbf{R}) = V(\mathbf{r})$. This does not mean that the Hamiltonian (3) commutes with the trans-

lation operator $\mathcal{T}_{\mathbf{R}} = \exp(\frac{i}{\hbar} \mathbf{R} \cdot \mathbf{p})$, since this translation shifts the argument of the vector potential. Since the vector potential $\mathbf{A}(\mathbf{r})$ describing the homogeneous magnetic field is linear in \mathbf{r} , this shift can be compensated by a gauge transformation $\mathcal{E}_{\mathbf{R}} = \exp[\frac{ie}{\hbar c} \mathbf{r} \cdot \mathbf{A}(\mathbf{R})]$, and the Hamiltonian commutes with the ‘‘magnetic translation operators’’ $\mathcal{M}_{\mathbf{R}} = \mathcal{E}_{\mathbf{R}} \mathcal{T}_{\mathbf{R}}$.⁴⁴ In general, the magnetic translations do not commute with each other. For the basis vectors one finds, for instance,

$$\mathcal{M}_{\mathbf{a}} \mathcal{M}_{\mathbf{b}} = \mathcal{M}_{\mathbf{b}} \mathcal{M}_{\mathbf{a}} \exp(-2\pi i \Phi / \Phi_0), \quad (10)$$

where $\Phi = a_x a_y B$ is the flux per unit cell of the superlattice; see Eq. (2). If the flux ratio is rational, $\Phi / \Phi_0 = p/q$, we may take $q\mathbf{a}$ and \mathbf{b} as the basis of an enlarged unit cell (magnetic unit cell) which is penetrated by an integer number p of flux quanta. Then, the magnetic translations corresponding to the Bravais lattice vectors $\mathbf{R}' = n(q\mathbf{a}) + m\mathbf{b}$ commute with each other and with the Hamiltonian. Thus, we choose eigenfunctions Ψ which diagonalize H and the $\mathcal{M}_{\mathbf{R}'}$ simultaneously. The eigenvalues of the basic magnetic translations are then given by

$$\mathcal{M}_{q\mathbf{a}} \Psi = e^{iqk_x a_x} \Psi, \quad \mathcal{M}_{\mathbf{b}} \Psi = e^{ik_y a_y} \Psi, \quad (11)$$

where k_x and k_y are generalized crystal momenta and can be restricted to the magnetic Brillouin zone (MBZ) $|k_x| \leq \pi/qa_x$, $|k_y| \leq \pi/a_y$. Periodic boundary conditions in the sense that *magnetic* translations in the x direction by L_x and in the y direction by L_y reproduce the wave functions are tacitly assumed, where $L_x = N_{qa} (qa_x) \rightarrow \infty$ and $L_y = N_b a_y \rightarrow \infty$ with integers N_{qa} and N_b . Then the spacing of the allowed k_y values is $\Delta k_y = 2\pi/L_y$ and that of the allowed k_x is $\Delta k_x = 2\pi/L_x$. Thus, the energy eigenvalues and eigenstates can be classified by the vector $\mathbf{k} = (k_x, k_y)$ in the MBZ, but may depend on an additional set of quantum numbers β . The number of \mathbf{k} vectors in the MBZ equals the number of magnetic unit cells in the sample, $N_{qa} N_b = L_x L_y / (qa_x a_y)$. The eigenfunction may be written in the Bloch form

$$\Psi_{\mathbf{k}}^{(\beta)}(x, y) = e^{ik_x x + ik_y y} u_{\mathbf{k}}^{(\beta)}(x, y). \quad (12)$$

In the Landau gauge we have $\mathcal{E}_{q\mathbf{a}} = \exp(ipK_y y)$ and $\mathcal{E}_{\mathbf{b}} = 1$, so that Eqs. (11) and (12) yield the properties

$$u_{\mathbf{k}}^{(\beta)}(x, y) = u_{\mathbf{k}}^{(\beta)}(x, y + b) = e^{ipK_y y} u_{\mathbf{k}}^{(\beta)}(x + qa, y). \quad (13)$$

The $u_{\mathbf{k}}^{(\beta)}(x, y)$ are eigenfunctions of the \mathbf{k} -dependent effective Hamiltonian $H(\mathbf{k})$ obtained from Eq. (3) by replacing \mathbf{p} with $\mathbf{p} + \hbar\mathbf{k}$. The components of the velocity operator are given in the space of these functions by

$$v_{\mu}(\mathbf{k}) = \hbar^{-1} \partial H(\mathbf{k}) / \partial k_{\mu} \quad (14)$$

with $\mu = x$ or y . We now substantiate these results by an explicit construction in the special case of our interest.

2. The Hofstadter-type spectrum

Following the work of Usov,³¹ we assume that the amplitudes $V_{\mathbf{g}}$ are so small that mixing of Landau levels by the superlattice potential can be neglected for the calculation of the energy spectrum.

The modulation in the y direction couples Landau states with center coordinates differing by integer multiples of $l^2 K_y$, so that the eigenstates can be written in the form

$$||n; \alpha\rangle\rangle = \sum_{\lambda=-\infty}^{\infty} c_{\lambda}(n, \alpha) |n, k_y + \lambda K_y\rangle. \quad (15)$$

To avoid double counting of states, we restrict k_y to the interval $|k_y| \leq K_y/2$. From the matrix elements (7), one obtains for the coefficients $c_{\lambda}(n, \alpha)$ the eigenvalue equation

$$\sum_{\lambda} \left\{ H_{\lambda', \lambda} - \tilde{E}_{n, \alpha} \delta_{\lambda', \lambda} \right\} c_{\lambda}(n, \alpha) = 0 \quad (16)$$

with the Hamilton matrix

$$H_{\lambda', \lambda} = \sum_{\mathbf{g}} \delta_{\lambda', \lambda + g_y/K_y} V_{\mathbf{g}} \mathcal{L}_n \left(\frac{l^2 g^2}{2} \right) \times \exp \left(-\frac{i}{2} l^2 g_x [2k_y + (\lambda' + \lambda) K_y] \right), \quad (17)$$

where the eigenvalues of H , Eq. (3), have been written as $E_{n, \alpha} = \hbar \omega_c (n + \frac{1}{2}) + \tilde{E}_{n, \alpha}$. Equation (16) is a generalization of Harper's equation,

$$[V_x \cos(\lambda l^2 K^2 - K x_0) - \varepsilon_{\alpha}] c_{\lambda}(\alpha) + \frac{V_y}{2} [c_{\lambda+1}(\alpha) + c_{\lambda-1}(\alpha)] = 0, \quad (18)$$

to which it reduces for the simple potential model (5) with $K_x = K_y = K$ and $V_{xy} = 0$. In this special case, only a single Laguerre polynomial factor occurs in (17), the energy eigenvalues can be written as $\tilde{E}_{n, \alpha} = \varepsilon_{\alpha} \mathcal{L}_n(\frac{1}{2} l^2 K^2)$, the $c_{\lambda}(n, \alpha)$ are independent of n , and all the LL's have the same internal energy structure determined by ε_{α} . In the following we call this the Hofstadter case.

If the commensurability condition (2) holds, the matrix (17) is periodic with period p , $H_{\lambda'+p, \lambda+p} = H_{\lambda', \lambda}$, since $l^2 K_x K_y p = 2\pi q$. That does not mean that the components $c_{\lambda}(\alpha)$ are periodic in λ with period p , but it allows the Bloch-type ansatz

$$c_{\lambda}(\alpha) = N_{qa}^{-1/2} e^{-ik_x l^2 (k_y + \lambda K_y)} u_{\lambda}(\mathbf{k}; j, n), \quad (19)$$

where the

$$u_{\lambda}(\mathbf{k}; j, n) = u_{\lambda+p}(\mathbf{k}; j, n) \quad (20)$$

now have this periodicity. The eigenstates of the n th LL then are labeled by the wave vector \mathbf{k} , defined in the MBZ, and by a subband index $j = 1, \dots, p$. There are N_{qa} allowed k_x values and N_b allowed k_y values in the MBZ, so that the total number of states per LL (and per

spin) is $p N_{qa} N_b = L_x L_y / (2\pi l^2)$, as it should be. For the discussion of the Hall conductivity, it is useful³¹ to introduce instead of the Landau states the new basis states

$$|n, \kappa; \mathbf{k}\rangle = N_{qa}^{-1/2} \sum_{t=-\infty}^{\infty} e^{-ik_x l^2 [k_y + (tp + \kappa) K_y]} \times |n; k_y + (tp + \kappa) K_y\rangle, \quad (21)$$

which satisfy in the MBZ the translation relations

$$|n, \kappa; k_x + K_x/q, k_y\rangle = e^{-i(\alpha_y k_y + \kappa)/p} |n, \kappa; k_x, k_y\rangle, \quad (22)$$

$$|n, \kappa; k_x, k_y + K_y\rangle = |n, \kappa + 1; k_x, k_y\rangle,$$

where κ is an integer modulo p , so that $|n, \kappa + p; \mathbf{k}\rangle \equiv |n, \kappa; \mathbf{k}\rangle$. They satisfy the eigenvalue equations (11) of the magnetic translation operators.

In order to have these simple symmetry properties, the t sum in Eq. (21) is extended from $-\infty$ to $+\infty$. In counting states, $tl^2 p K_y$ is restricted to an interval of length L_x , i.e., to L_x/qa_x different t values. The corresponding Landau states are mapped by the unitary transformation (21) onto the states $|n, \kappa; \mathbf{k}\rangle$ with k_x and (the fixed) k_y in the MBZ.

It is easy to show that matrix elements of the potential (4), and thus of the Hamiltonian (3), in the basis (21) are diagonal in \mathbf{k} , but in general not in the n and κ quantum numbers. In the first-order approximation of Eqs. (16) and (17), where mixing of the LL's by the superlattice potential is neglected, the energy eigenstates (15) can be written as

$$||n; j, \mathbf{k}\rangle\rangle = \sum_{\kappa=1}^p u_{\kappa}(\mathbf{k}; j, n) |n, \kappa; \mathbf{k}\rangle. \quad (23)$$

Here the $u_{\kappa}(\mathbf{k}; j, n)$, $j = 1, \dots, p$, satisfy Eqs. (19) and (20), and form the components of the normalized eigenvector $\mathbf{u}^{(p)}(\mathbf{k}; j, n)$ of the $p \times p$ effective Hamiltonian matrix

$$[h^{(p)}(\mathbf{k})]_{\kappa', \kappa} = \sum_{\mathbf{g}} \tilde{\delta}_{[g_y/K_y], \kappa' - \kappa}^{(p)} V_{\mathbf{g}} \mathcal{L}_n \left(\frac{l^2 g^2}{2} \right) \times \exp[-il^2 (g_x k_y - g_y k_x + \kappa g_x K_y + \frac{1}{2} g_x g_y)] \quad (24)$$

with energy eigenvalue $\tilde{E}_{n, j}(\mathbf{k})$. Here $[g_y/K_y]$ means g_y/K_y modulo p , i.e., the integer satisfying $1 \leq [g_y/K_y] \leq p$ and $g_y/K_y = N_y p + [g_y/K_y]$, where N_y is an integer, and

$$\tilde{\delta}_{[g_y/K_y], \kappa' - \kappa}^{(p)} = \begin{cases} 1 & \text{if } [g_y/K_y] = \kappa' - \kappa \text{ or } \kappa' - \kappa + p \\ 0 & \text{otherwise.} \end{cases} \quad (25)$$

For $p=1$, i.e., if a single flux quantum threads q unit cells of the superlattice, the eigenvalues of the Hamiltonian matrix (24) form a single Landau band,

$$\tilde{E}_n^{(1)}(\mathbf{k}) = \sum_{\mathbf{g}} V_{\mathbf{g}} e^{-i l^2 (g_x k_y - g_y k_x + \frac{1}{2} g_x g_y)} \mathcal{L}_n(\frac{1}{2} l^2 g^2). \quad (26)$$

It is interesting to compare this result with the classical average of the potential (4) over the cyclotron orbit with radius R_n and center at \mathbf{r}_0 ,

$$\tilde{E}^{cl}(\mathbf{r}, R_n) = \sum_{\mathbf{g}} V_{\mathbf{g}} e^{i \mathbf{g} \cdot \mathbf{r}_0} J_0(g R_n), \quad (27)$$

which reduces in the limit of very strong magnetic fields ($B \rightarrow \infty$) to $\tilde{E}^{cl}(\mathbf{r}_0, 0) = V(\mathbf{r}_0)$. With the suggestive notation $-l^2 k_y = x_0$ and $l^2 k_x = y_0$, and with the asymptotic equality (9), Eq. (26) becomes very similar to the classical result (27). For the simple model (5) one obtains, for instance,

$$\begin{aligned} \tilde{E}_n^{(1)}(\mathbf{k}) = & \tilde{V}_x \cos(K_x x_0) + \tilde{V}_y \cos(K_y y_0) \\ & + (-1)^q \tilde{V}_{xy} \cos(K_x x_0) \cos(K_y y_0), \end{aligned} \quad (28)$$

where $\tilde{V}_x = V_x \mathcal{L}_n(l^2 K_x^2/2)$, $\tilde{V}_y = V_y \mathcal{L}_n(l^2 K_y^2/2)$, and $\tilde{V}_{xy} = V_{xy} \mathcal{L}_n(l^2 [K_x^2 + K_y^2]/2)$. There are two important differences between the quantum-mechanical results (26) and (28) and the corresponding classical formula (27). First, $\mathbf{k} = (k_x, k_y)$ is restricted to the MBZ. Second, the quantum result contains a phase factor $\exp(-\frac{i}{2} l^2 g_x g_y)$, which is $+1$ or -1 if the integer $l^2 g_x g_y / (2\pi)$ is even or odd (note that $p = 1$). This is a consequence of the Bragg reflections. In contrast to the case of a 1D superlattice, the classical high- B approximation is not applicable to the case of a 2D superlattice (if its periods are much smaller than the phase coherence length).

For $p > 1$, each Landau level splits into p subbands, which can be shown to be q -fold degenerate.³¹ For $p = 2$ the energy eigenvalues can easily be obtained analytically. The result for the simple model (5) is

$$\begin{aligned} \tilde{E}_{n,j}^{(2)} = & (-1)^j \left[\tilde{V}_x^2 \cos^2\left(\frac{q}{2} k_y a_y\right) + \tilde{V}_y^2 \cos^2\left(\frac{q}{2} k_x a_x\right) \right. \\ & \left. + \tilde{V}_{xy}^2 \sin^2\left(\frac{q}{2} k_x a_x\right) \sin^2\left(\frac{q}{2} k_y a_y\right) \right]^{\frac{1}{2}}. \end{aligned} \quad (29)$$

If $V_x V_y V_{xy} \neq 0$, the two subbands are separated by a gap of finite width. For $V_{xy} = 0$ the subbands touch each other (at the corners of the MBZ).⁴⁵

The energy spectrum is best studied for the Hofstadter case [see Eq. (18)], where the factorization $\tilde{E}_{n,j}^{(p)}(\mathbf{k}) = \varepsilon(\mathbf{k}; j) \mathcal{L}_n(\frac{1}{2} l^2 K^2)$ leads to the same internal subband structure for all LL's, but with a B - and n -dependent modulation of the bandwidth given by Eq. (9) with $q = 2\pi/a$. In Fig. 1 we show the ranges of allowed energy values

$$E_n = \hbar \omega_c (n + \frac{1}{2}) + \varepsilon \mathcal{L}_n(\frac{1}{2} l^2 K^2) \quad (30)$$

for $|\varepsilon| \leq 0.2$ meV as dark areas. The "flat band energies" $\varepsilon_\lambda = \frac{1}{8} m \omega_c^2 a^2 (\lambda - \frac{1}{4})^2$, i.e., the energies of cyclotron orbits with radii R_c satisfying the commensurability condition

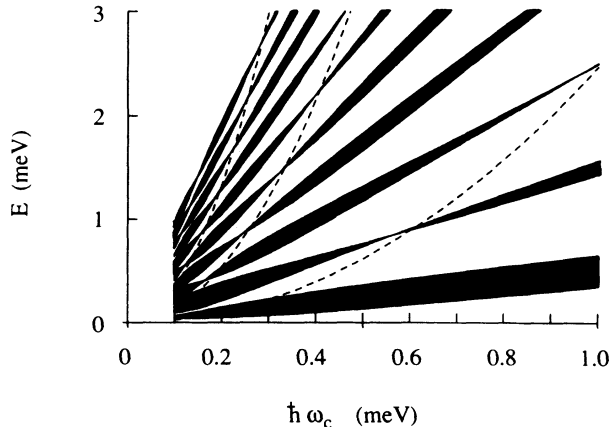


FIG. 1. Sketch of the modulation-broadened Landau fan diagram, calculated from Eq. (30) with $|\varepsilon| \leq 0.2$ meV and $2\pi/K = 200$ nm. Allowed energy regions in the Landau bands with $n = 0, 1, \dots, 9$ are darkened. The approximate flat band energies ε_λ , calculated from the asymptotic form (9), are shown for $\lambda = 1, 2, 3$ as dashed lines.

(1), are indicated by the dashed parabolas for $\lambda = 1, 2$, and 3. They intersect the Landau fan at the zeros of the cosine in Eq. (9), i.e., for large n , at the flat band situations.

If the allowed $\varepsilon(\mathbf{k}; j)$ are plotted versus the ratio q/p of Eq. (2), i.e., versus the inverse number of flux quanta per unit cell of the superlattice, one obtains the self-similar pattern^{30,46,47} shown in Fig. 2, which is known as Hofstadter's butterfly.²⁹ The apparent symmetry of the pattern under the exchange of $1 - q/p$ with q/p is easily proven analytically. For $q/p > 1$, the pattern repeats itself periodically with period unity, so that the interval $0 < q/p \leq 1$ contains all relevant information. An interesting and important property of the butterfly is the

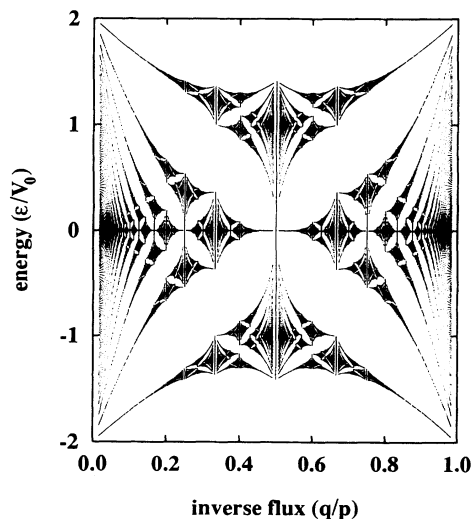


FIG. 2. Hofstadter's butterfly, showing the intervals of allowed values for the eigenvalue ε_α of Harper's Eq. (18), in units of $V_0 = V_x = V_y$, for rational values of the flux ratio $\Phi/\Phi_0 = p/q$, as a function of q/p .

clustering of bands into groups. For a given flux ratio p_0/q_0 , one gets p_0 bands. For a rational value p/q close to p_0/q_0 , one gets p bands which group themselves into p_0 clusters close to the p_0 bands of the previous case. The band gaps obtained for the previous case remain free of allowed energies in intervals of finite width.^{46,47}

If a series of rational values q/p converges towards an irrational number σ , the number of narrow gaps increases in such a way that the probability of finding gaps of width less than δ diverges as δ approaches zero.⁴⁸

Some of these features are illustrated in Fig. 3, which shows calculated energy bands in (one-quarter of) the MBZ. The flux ratio is $p/q = 3$ and $3/4$ in Figs. 3(a) and 3(b), respectively, so that we obtain three bands in both cases. The energy spectrum in (b) is $q =$ fourfold degenerate (four periods in the k_y direction), however its projection onto the energy axis is identical to that of the spectrum in (a). This illustrates the periodicity of the Hofstadter plot as a function of q/p with period 1. The comparison of (c) with (a) illustrates the clustering. For a flux ratio $p/q = 10/3$ (close to $p_0/q_0 = 3/1$) one obtains ten subbands which cluster into three groups, the inner one containing four subbands and the outer ones containing three subbands each. The projections of the subbands onto the energy axis yield ten intervals (the two innermost are connected) which cluster into three groups, each of which is located in the close neighborhood of one of the three intervals obtained for the flux ratio $p_0/q_0 = 3/1$; see Fig. 2. We have also calculated the bands for $p/q = 11/4$, and obtained again three well-separated clusters of subbands, the inner one containing three and the outer ones each containing four narrow subbands (cf. Fig. 2 for $q/p = 4/11$). On the other hand, no pronounced clustering of the subbands is obtained for integer values of the flux ratio, e.g., $p/q = 10$ or 11.

If the Fourier expansion (4) of the superlattice potential contains contributions with different values of $|g|$, e.g., for a rectangular lattice with $a_x \neq a_y$ or for the

model (5) with $V_{xy} \neq 0$, the Laguerre polynomials cannot be factorized out from the matrix (24). Then the internal structure is different in different LL's, and a highly symmetric representation of the energy spectrum as by Hofstadter's butterfly is not possible. This situation is clarified in Figs. 4 and 5. Figure 4 shows for the Hofstadter case, Eq. (5) with $K_x = K_y = K$, $V_x = V_y$, and $V_{xy} = 0$, the eigenvalue spectrum of the Hamiltonian matrix (24) for the LL's $n = 0$ and 1. The only difference from a periodic continuation of the butterfly of Fig. 2 is due to the Laguerre factors $\mathcal{L}_n(\frac{1}{2}K^2l^2)$. For $n = 1$, this factor vanishes if $\frac{1}{2}K^2l^2 = 1$. This leads to zero bandwidth for $p/q \rightarrow \pi$. In general, the \mathcal{L}_n are oscillatory functions of n . According to Eq. (9) the zeros, i.e., vanishing bandwidth, are given by Eq. (1) with $R_c = R_n$.

The corresponding spectra for the case $V_{xy} = V_x = V_y$ are shown in Fig. 5. Now the diagonal and the off-diagonal matrix elements of the effective Hamiltonian (24) [or (17)] contain Laguerre factors with different arguments, so that their ratio depends on the flux ratio Φ/Φ_0 and cannot be factorized out.

The occurrence of Laguerre polynomial factors is specific for the situation of our interest. They result from the matrix elements of the weak periodic potential in the Landau basis. In the tight-binding approach one starts with a periodic $\varepsilon(\mathbf{k})$ relation. The Peierls substitution then leads to a set of difference equations, but no such flux-dependent Laguerre polynomial factors occur, and a highly symmetric energy spectrum results. Claro⁴⁹ has investigated a model with next-to-nearest-neighbor interaction, which is the tight-binding analog of our model (5). He found a highly symmetric, self-similar energy spectrum similar to Hofstadter's butterfly, although without reflection symmetry. This lowering of the symmetry is due to the presence of higher harmonics of the superlattice potential. The periodic dependence on the flux ratio now has a period which is twice as large as in the

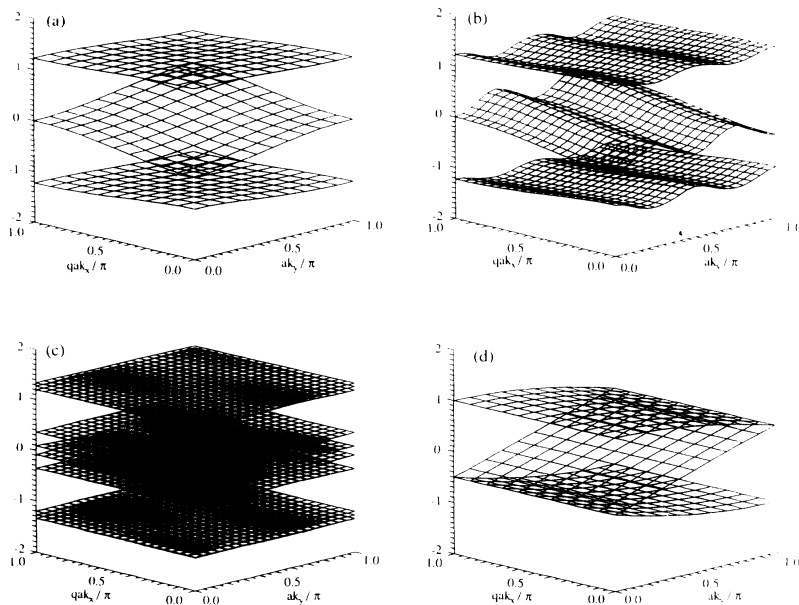


FIG. 3. Energy bands over one-quarter of the magnetic Brillouin zone. The scaled energy values $\varepsilon(\mathbf{k}, j)$ (without the Laguerre factors; see the text) are plotted in units of V_x , (a)–(c) for the Hofstadter case $V_y = V_x$ and for the values $p/q = 3/1$ (a), $3/4$ (b), $10/3$ (c) of the flux ratio, and (d) for a 1D superlattice ($V_y = 0$) and $p/q = 3/1$.

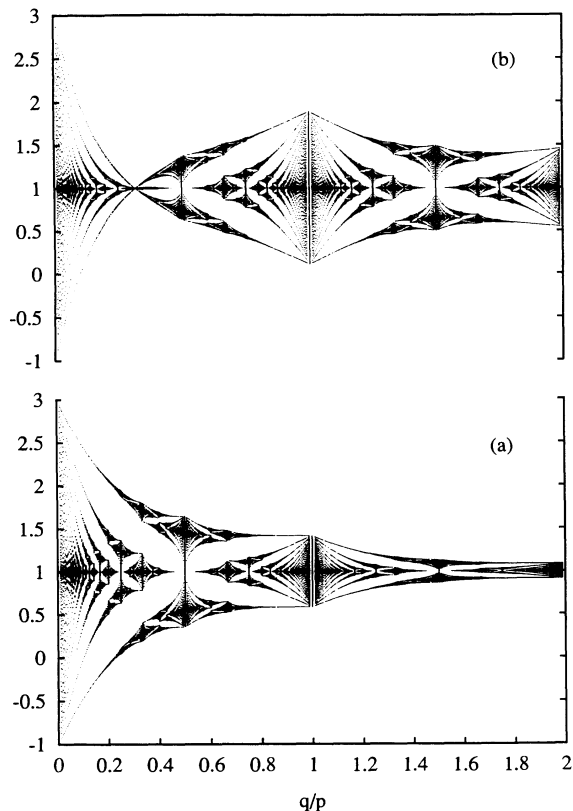


FIG. 4. Allowed values for the energy correction $\tilde{E}_{n,\alpha}$ (in units of V_0) to the n th Landau energy owing to the superlattice potential $V(x, y) = V_0[1 + \cos Kx + \cos Ky]$, versus rational values of the inverse flux ratio $l^2 K^2 / 2\pi \equiv \Phi_0 / \Phi = q/p$; (a) for $n = 0$, (b) for $n = 1$.

Hofstadter case.

In our weak-modulation limit this periodicity is obscured by the Laguerre polynomial factors. The factor $(-1)^q$ in Eq. (28) is indicative of this reduced periodicity. Note that in Fig. 5 the width of the $n = 1$ Landau band does not vanish for any B value, since the Laguerre factors with different arguments do not vanish simultaneously.

The inclusion of higher harmonics of the superlattice potential thus alters the details of the energy spectrum. Qualitatively, however, the complicated fractal structure and especially a pronounced subband splitting remains. Similar complicated energy spectra have recently been obtained for a lattice model of electrons in a quantum dot⁵⁰ and for a finite array of coupled quantum dots.⁵¹ In those 2D ES's the gap structure is, however, partially obscured by edge states.⁵²

Of course the same formalism can be used to describe a 1D superlattice in the x direction only. Then the effective Hamiltonian (24) is diagonal and independent of k_x , and $u_\lambda(\mathbf{k}; j) = \delta_{\lambda,j}$. The energy eigenvalues are independent of k_x , and the j bands are just a backfolding of the simple 1D band into the MBZ. For the Hofstadter case with $V_y = 0$, the sum over j restores q periods of $V_x \cos(Kx_0)$.⁸ For a flux ratio $p/q = 3$, the corresponding band structure

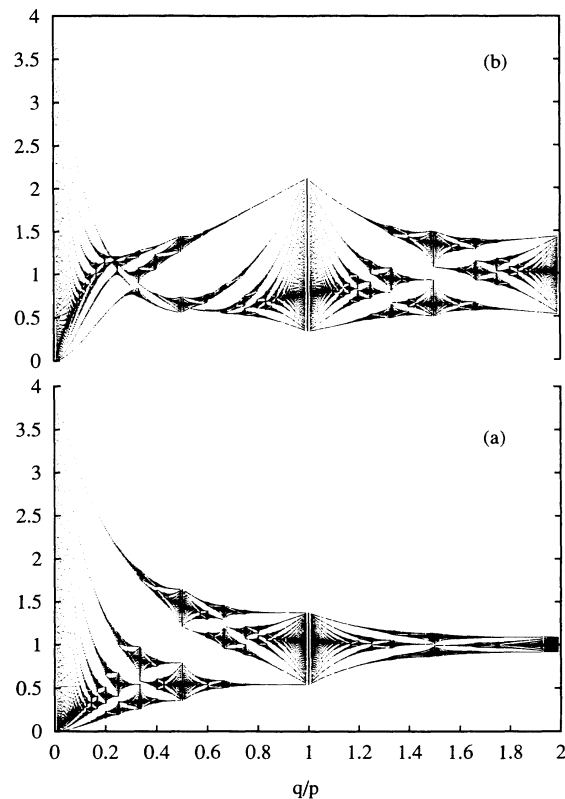


FIG. 5. The same as Fig. 4, but for the superlattice potential $V(x, y) = V_0(1 + \cos Kx)(1 + \cos Ky)$.

is plotted in Fig. 3(d). Comparison with Fig. 3(a) shows that, for $V_y \rightarrow 0$, the gaps between the subbands close at integer values of ak_y/π .

3. Group velocities

The matrix elements of the velocity operator taken with the zeroth-order states given by Eqs. (15) and (19) yield

$$\begin{aligned} \langle \langle n, j; \mathbf{k} | v_\mu | n', j'; \mathbf{k}' \rangle \rangle \\ = \delta_{\mathbf{k}, \mathbf{k}'} \delta_{j, j'} \frac{l\omega_c}{\sqrt{2}} \left[\sigma_\mu \sqrt{n+1} \delta_{n', n+1} + \sigma_\mu^* \sqrt{n} \delta_{n', n-1} \right], \end{aligned} \quad (31)$$

with $\sigma_x = i$ and $\sigma_y = 1$, independent of the modulation amplitude. To improve on this, one has to calculate the eigenstates to first order in the modulation potential,

$$\begin{aligned} | | n, j; \mathbf{k} \rangle \rangle = | | n, j; \mathbf{k} \rangle \rangle \\ + \sum_{n' \neq n, j'} \frac{\langle \langle n', j'; \mathbf{k} | V | n, j; \mathbf{k} \rangle \rangle}{\hbar\omega_c(n - n')} | | n', j'; \mathbf{k} \rangle \rangle. \end{aligned} \quad (32)$$

From these states one finds that the velocity operator has nonvanishing intra-LL ($n' = n$) matrix elements, which

are proportional to the amplitude of the modulation and can be calculated from the eigenvectors $\mathbf{u}^{(p)}(\mathbf{k}; j, n)$, Eq. (23), and the $p \times p$ matrices^{30,15}

$$\left[v_{\mu}^{(p)}(\mathbf{k}; n) \right]_{\kappa', \kappa} = \frac{1}{\hbar} \frac{\partial}{\partial k_{\mu}} \left[h^{(p)}(\mathbf{k}; n) \right]_{\kappa', \kappa}, \quad (33)$$

where $\mu = x, y$. If the potential (4) is of the form $V(x, y) = V_x(x) + V_y(y)$, e.g., as the model (5) with $V_{xy} = 0$, then the matrix $v_{\mu}^{(p)}(\mathbf{k})$ is independent of the modulation V_{μ} in the μ direction and depends only on the modulation in the other direction, just as the classical drift velocity. Apparently Eq. (33) is a generalization of the Feynman-Hellmann theorem, which applies only to the diagonal matrix elements $(n, j; \mathbf{k} | v_{\mu} | n, j; \mathbf{k})$.

III. DENSITY OF STATES

The influence of randomly distributed impurities is usually discussed in the Green's-function formalism. While the impurity potential acting on an electron at \mathbf{r} ,

$$V_I(\mathbf{r}) = \sum_j u(\mathbf{r} - \mathbf{R}_j) = \sum_j u_{R_j}(\mathbf{r}), \quad (34)$$

depends on the specific impurity configuration $\{\mathbf{R}_j\}$, macroscopic quantities can be expressed by an average over all configurations.

The impurity averaged Green's-function operator,

$$G(z) = \langle \mathcal{G}(z) \rangle_{\text{imp}} = \left\langle \frac{1}{z - H - V_I} \right\rangle_{\text{imp}}, \quad (35)$$

satisfies Dyson's equation with the self-energy operator $\Sigma(z)$, and thus can be written as

$$G(z) = \frac{1}{z - H - \Sigma(z)}. \quad (36)$$

In the self-consistent Born approximation (SCBA),^{53,54,36} $\Sigma(z)$ is taken proportional to the averaged Green's-function operator,

$$\Sigma(z) = n_I \int d^2 R u_R G(z) u_R, \quad (37)$$

where n_I denotes the impurity concentration and $\langle \mathbf{r} | u_R \rangle = u(\mathbf{r} - \mathbf{R})$. Equations (36) and (37) form a set of self-consistency equations for the Green's-function operator $G(z)$.

As has been discussed by Zhang and Gerhardt⁸ for the case of a unidirectional modulation, the solution of this set of equations is complicated by the fact that the operators Σ and G neither commute with each other nor with the Hamiltonian H , Eq. (3), containing the superlattice potential but not the disorder. Thus, in contrast to the unmodulated system, there exists no representation in which both Σ and G are diagonal. The only obvious symmetry of the impurity-averaged system is the invariance under the magnetic translations, which implies that both G and Σ are diagonal with respect to the quantum numbers \mathbf{k} in the MBZ.

We do not attempt to calculate the complicated quantum number dependence of the self-energy. Instead, we follow Ref. 8 and make the ansatz of a quantum-number independent self-energy defined by the self-consistency requirement

$$\begin{aligned} \Sigma(z) &= \Gamma_0^2 \frac{2\pi l^2}{L_x L_y} \text{tr} G(z) \\ &= \sum_{n,j} \int d^2 k \frac{\Gamma_0^2 l^2 / 2\pi}{z - E_{n,j}(\mathbf{k}) - \Sigma(z)}. \end{aligned} \quad (38)$$

Here a high-energy cutoff $n < 2E_F/\hbar\omega_c$ is implied to make $\text{Re}\Sigma$ finite and to guarantee the analyticity of $G(z)$ in the upper $[G^+(z)]$ and the lower $[G^-(z)]$ complex halfplane.^{8,53,54} Since $\Sigma(z)$ is assumed to be a c number (a multiple of the unity operator), $G(z)$ commutes with H and is diagonal in the $|n, j; \mathbf{k}\rangle$ representation, Eq. (23). The simplified ansatz (38) still contains the essence of a description of collision broadening effects in the SCBA. For vanishing modulation $[V(x, y) \equiv 0]$ and short-range impurities $[u(\mathbf{r}) = U_0\delta(\mathbf{r})]$ it becomes identical to the SCBA result with

$$\Gamma_0^2 = \frac{1}{2\pi} \hbar\omega_c \frac{\hbar}{\tau}, \quad (39)$$

where τ denotes the corresponding lifetime for zero magnetic field.³⁶

The density of states (DOS) is given by

$$D(E) = 2 \sum_n D_n(E) = \frac{2}{(2\pi)^2} \sum_{n,j} \int d^2 k A_{n,j;\mathbf{k}}(E), \quad (40)$$

where $A(E) = \pi^{-1} \text{Im}G^-(E)$ is the spectral function, and the factor 2 takes care of the spin degeneracy. From Eq. (38) one obtains

$$\text{Im}\Sigma^-(E) = [\pi l \Gamma_0]^2 D(E), \quad (41)$$

i.e., the width of the spectral function itself is directly proportional to the DOS. This result is typical for the SCBA and reflects the mixing of LL's by the (short-range) impurity scattering. As a consequence, the spectral function $A_{n,j;\mathbf{k}}(E)$ has side peaks at the other Landau levels $n' \neq n$, i.e., the probability to find an electron in state $|n, j; \mathbf{k}\rangle$ at energy E is nonzero where $D(E) \neq 0$. The existence of such side peaks of the spectral functions is by no means an artifact of the SCBA. Other consistent treatments of multiple scattering by finite-range impurity potentials lead to similar results.⁵⁵ The existence of these side peaks will become important in the following.

Figure 6 shows the DOS for a modulated system with a unidirectional (a) and a two-dimensional (b) lateral superlattice, as a function of the magnetic field B and the energy E .⁵⁶ In both cases the (n -dependent) oscillatory width of the Landau bands results in an amplitude oscillation of the DOS. But, while the intraband structure in the 1D modulation potential is just due to van Hove singularities at the band edges,⁸ the 2D modulated DOS reveals the rich subband structure of the Hofstadter-type energy spectrum. Moreover, a general result becomes ev-

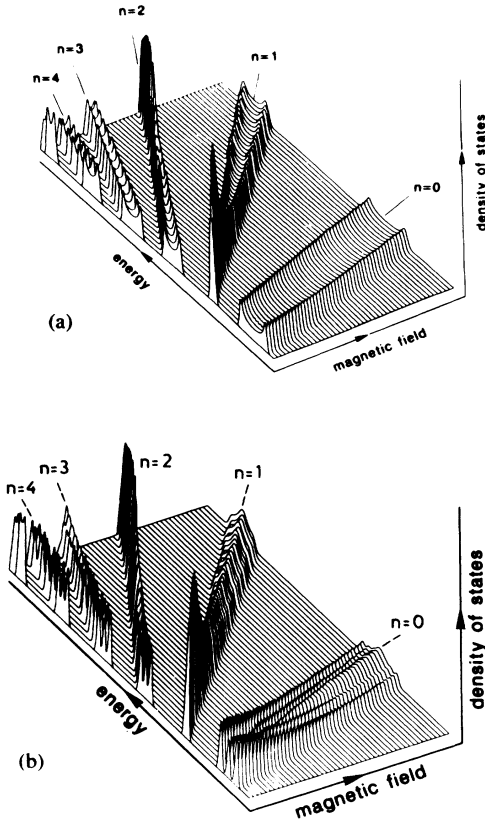


FIG. 6. Density of states for a superlattice potential of the form $V(x, y) = V_x \cos Kx + V_y \cos Ky$, and a collision broadening $\Gamma_0 = 0.035\sqrt{B}$ [T] meV, for $0.5 \leq B \leq 1.65$ T and $0 \leq E \leq 5$ meV, for (a) a grating modulation with $V_x = 0.5$ meV, $V_y = 0$ and (b) a grid modulation with $V_x = V_y = 0.25$ meV.

ident: Collision broadening effectively smears out the fine structure due to the many subbands resulting from large p (and large q) values. In spite of the highly singular B dependence of the energy spectrum, the DOS appears as a continuous function of the magnetic field. This was also observed in CPA calculations in the strong-modulation tight-binding limit.⁵⁷ For small values $p/q \sim 3-5$, single clusters of subbands can be resolved in widely broadened bands ($n = 1, B = 0.5 - 1.0$ T), while for larger fluxes per unit cell even these clusters grow together and form one single Landau band.

IV. CONDUCTIVITIES

A. Consistent treatment of collision broadening

According to Kubo's formula^{58,54} the static conductivity tensor is given by

$$\sigma_{\mu\nu} = \frac{4e^2\hbar}{L_x L_y} \int_{-\infty}^{\infty} dE f(E) \times \text{Im tr} \left\langle \delta(E - H) v_\nu \frac{d\mathcal{G}^-(E)}{dE} v_\mu \right\rangle_{\text{imp}}. \quad (42)$$

Since

$$\delta(E - H) = \frac{1}{2\pi i} [\mathcal{G}^-(E) - \mathcal{G}^+(E)], \quad (43)$$

the impurity average is described by the operator

$$F(z, z'; v_\mu) = \langle \mathcal{G}(z) v_\mu \mathcal{G}(z') \rangle_{\text{imp}}, \quad (44)$$

which has to be evaluated in a manner consistent with the approximation Eq. (38) for the self-energy. This means that the approximation scheme for the evaluation of transport coefficients is already determined by the approximation chosen for the self-energy. Stated in simple terms, this means that identities such as

$$\mathcal{G}(z) v_\mu \mathcal{G}(z) = \frac{i}{\hbar} [\mathcal{G}(z), r_\mu] \quad (45)$$

and

$$\mathcal{G}(z) \mathcal{G}(z') = -[\mathcal{G}(z) - \mathcal{G}(z')]/(z - z'), \quad (46)$$

which follow immediately from $v_\mu = i[H, r_\mu]/\hbar$ and the analytic structure of the resolvent operator $\mathcal{G}(z) = (z - H - V_I)^{-1}$, must remain valid after taking the configuration average over the impurity distribution on both sides of the equations. Thus, the response quantity (44), being the average of a product containing two \mathcal{G} factors, is directly related to the Green's function $G(z)$, Eq. (35), i.e., the average of $\mathcal{G}(z)$ itself. Exploiting the analytical structure of $G(z)$, we may write the impurity-averaged Eqs. (45) and (46) as

$$F(z, z; v_\mu) = G(z) \left\{ v_\mu + \frac{i}{\hbar} [\Sigma(z), r_\mu] \right\} G(z) \quad (47)$$

and

$$F(z, z'; 1) = G(z) \left\{ 1 - \frac{\Sigma(z') - \Sigma(z)}{z' - z} \right\} G(z'). \quad (48)$$

In fact these identities are limiting cases of the more general Ward identities relating self-energy and irreducible vertex part in the standard many-body perturbation theory. In the SCBA, the Bethe-Salpeter equation reads

$$F(z, z'; v_\mu) = G(z) \left(v_\mu + n_I \int d^2R u_R F(z, z'; v_\mu) u_R \right) G(z'), \quad (49)$$

and the identities (47) and (48) are satisfied by its solution.^{53,54}

Our simplified treatment of collision broadening effects can formally be obtained from the SCBA by the replacement

$$n_I \int d^2R u_R \mathcal{O} u_R = \gamma^2 (\text{tr } \mathcal{O}) \mathbf{1} \quad (50)$$

for any operator \mathcal{O} . Here $\mathbf{1}$ is the unity operator and $\gamma^2 = \Gamma_0^2 2\pi l^2 / L_x L_y$.

For $\mathcal{O} = G(z)$, Eq. (38) results from Eq. (37). With $\mathcal{O} = F(z, z'; v_\mu)$, Eq. (49) yields

$$F(z, z'; v_\mu) = G(z) v_\mu G(z'), \quad (51)$$

since

$$\text{tr } F(z, z'; v_\mu) = \frac{\text{tr } G(z) v_\mu G(z')}{1 - \gamma^2 \text{tr } G(z) G(z')} = 0. \quad (52)$$

The numerator vanishes as a simple consequence of $v_\mu = i[H, r_\mu]/\hbar$ and $[G(z), H] = 0$, which holds in the approximation (38). Thus, current vertex corrections vanish in our approximation, and identity (47) is trivially satisfied since, according to Eq. (38), $\Sigma(z) \propto \mathbf{1}$ and $[\Sigma, r_\mu] = 0$.

The identity (48) is also satisfied since

$$\begin{aligned} \gamma^2 \text{tr } F(z, z'; \mathbf{1}) &= \frac{\gamma^2 \text{tr } G(z) G(z')}{1 - \gamma^2 \text{tr } G(z) G(z')} \\ &= -\frac{\Sigma(z') - \Sigma(z)}{z' - z}, \end{aligned} \quad (53)$$

where the first equality follows from our approximation

$$\sigma_{\mu\mu}(E) = \frac{e^2 \hbar}{2\pi} \int d^2 k \sum_{n, n'} \sum_{j, j'} |((n'; \alpha' | v_\mu | n; \alpha))|^2 A_{n\alpha}(E) A_{n'\alpha'}(E) \quad (55)$$

with $\alpha = (\mathbf{k}; j)$ and $\alpha' = (\mathbf{k}; j')$. For the Hall conductivity one obtains

$$\sigma_{yx} = \frac{e^2 \hbar}{\pi^2} \int_{-\infty}^{\infty} dE f(E) \int d^2 k \text{Im} \left[\sum_{n, n'} \sum_{j, j'} A_{n\alpha}(E) ((n, \alpha | v_x | n', \alpha')) ((n', \alpha' | v_y | n, \alpha)) \frac{dG_{n'\alpha'}^-}{dE} \right]. \quad (56)$$

Here we have taken into account that the velocity matrix elements are diagonal in \mathbf{k} .

In the following we distinguish two contributions to the conductivity, $\sigma_{\mu\mu}(E) = \sigma_{\mu\mu}^{\text{sc}}(E) + \Delta\sigma_{\mu\mu}(E)$. The ‘‘band conductivity’’ $\Delta\sigma_{\mu\mu}(E)$ arises from the intra-Landau-band ($n' = n$) part of the above sum, which diverges in the absence of the random scatterers and vanishes for the unmodulated system. The ‘‘scattering conductivity’’ $\sigma_{\mu\mu}^{\text{sc}}(E)$ arises from impurity-induced scattering of electrons between different Landau levels ($n' \neq n$) and is the only contribution in the more familiar unmodulated case.

B. Band conductivity

The magnitude of the band conductivity $\Delta\sigma_{\mu\mu}(E)$ is determined by two factors which depend significantly on the Landau-band index n and the modulation-induced bandwidth. First, there are the velocity matrix elements $((n; \alpha' | v_\mu | n; \alpha))$ which, according to Eq. (33), are proportional to the amplitudes $V_{\mathbf{g}}$ of the superlattice potential and, thus, to the effective modulation-induced width of the n th Landau band. The second factor, the product of the spectral functions, depends also on the modulation-induced broadening of the Landau level and its subband splitting, but also in a delicate manner on the collision broadening due to random impurity scattering. If the collision broadening ($\propto \Gamma_0$) is so small that the modulation-induced subband splitting is (partially) resolved, then the magnitude of $\Delta\sigma_{\mu\mu}(E)$ becomes much smaller than in the opposite situation, where this sub-

band splitting is totally smeared out by collision broadening effects. We first discuss this latter situation.

According to this result the δ function in Kubo’s formula (42) has to be replaced by the spectral function $A(E)$ and the nonaveraged Green’s functions by the appropriate averaged ones, which have been discussed in Sec. III. Integrating by parts and choosing the energy representation of the modulated system, the diagonal components of the conductivity tensor can be written as

$$\sigma_{\mu\mu} = \int dE \left(-\frac{df(E)}{dE} \right) \sigma_{\mu\mu}(E), \quad (54)$$

where $f(E)$ denotes the Fermi function and $\sigma_{\mu\mu}$ is given by

band splitting is totally smeared out by collision broadening effects. We first discuss this latter situation.

1. Quasiclassical limit

Here we neglect the effect of the superlattice potential on the spectral functions, i.e., we replace the energy eigenvalues $E_{n;\alpha}$ by $\hbar\omega_c(n + \frac{1}{2})$ and thus neglect the subband splitting of the LL’s, which is of a quantum-mechanical origin. This quasiclassical approximation, $A_{n\alpha}(E) A_{n'\alpha'}(E) \approx [A_n(E)]^2$, is justified only for sufficiently large collision broadening. It allows us to evaluate the summation over the internal quantum numbers α, α' analytically, as is shown in Appendix A. The sum over j and j' reduces to a trace of a $p \times p$ matrix,

$$\sum_{j, j'} |((n; \alpha' | v_\mu | n; \alpha))|^2 = \text{tr}^{(p)} [v_\mu^{(p)}(\mathbf{k}; n)]^2, \quad (57)$$

which can be evaluated in the representation (33) using Eq. (24). The sum over κ, κ' and integration over the MBZ result in a Kronecker $\delta_{\mathbf{g}', \mathbf{g}}$, reducing the Fourier sums of the two v_μ factors to a single sum, with the result

$$\Delta\sigma_{\mu\mu}^{\text{qcl}}(E) = \frac{e^2 l^2}{\hbar} \sum_n \sum_{\mathbf{g}} \left| \bar{g}_\mu \tilde{V}_{\mathbf{g}}^{(n)} A_n(E) \right|^2, \quad (58)$$

where $\bar{g}_x = -g_y$, $\bar{g}_y = g_x$, and $\tilde{V}_{\mathbf{g}}^{(n)} = V_{\mathbf{g}} \mathcal{L}_n(\frac{1}{2} l^2 g^2)$. This is the extension to a 2D superlattice of a formula derived recently¹² for a 1D situation. In the typical quasi-

classical situation one has many LL's occupied, i.e., the Fermi energy is $E_F \approx \hbar\omega_c(n_F + \frac{1}{2})$ with $n_F \gg 1$, the LL's have small collision broadening, $\hbar\omega_c/\Gamma_0 = \tau\omega_c \gg 1$, but the LL's are smeared out by thermal broadening. Then, in the spirit of the SCBA, where $A_n(E) = (\pi\Gamma_0)^{-1}[1 - (E - E_n)^2/4\Gamma_0^2]^{1/2}$, one may for $k_B T \gg \Gamma_0$ approximate $\int dE f'(E)[A_n(E)]^2 \approx f'(E_n)/\Gamma_0\pi$ and replace the Laguerre polynomial by its large index approximation, cf. Eq. (9). This yields

$$\Delta\sigma_{\mu\mu}^{\text{qcl}} = \frac{e^2 l^2}{\pi\hbar\Gamma_0} \sum_n [-f'(E_n)] \sum_{\mathbf{g}} |\bar{g}_\mu V_{\mathbf{g}} J_0(gR_n)|^2. \quad (59)$$

Replacing the n sum by an integral over E_n and $-f'(E)$ by $\delta(E - E_F)$, one obtains

$$\Delta\sigma_{\mu\mu}^{\text{qcl}} = \frac{\tau e^2}{\pi m (\hbar\omega_c)^2} \sum_{\mathbf{g}} \bar{g}_\mu^2 |V_{\mathbf{g}}|^2 [J_0(gR_c)]^2, \quad (60)$$

with $R_c = R_n$ at $n = n_F$. This is a good approximation if the n dependence of the J_0 term near the Fermi level for the relevant Fourier coefficients is sufficiently weak, i.e., to lowest order in the small parameter $k_B T g R_c / E_F \ll 2\pi$. The result (60) can be obtained by a classical calculation taking into account the effect of the guiding-center drift of cyclotron orbits in the weak lateral superlattice potential.¹² This classical nature of the band conductivity was emphasized by Beenakker⁵ for the special case of a 1D superlattice. For a unidirectional simple cosine potential and with the asymptotic expression (9), Eq. (60) assumes the form first given explicitly by Winkler, Kotthaus, and Ploog.³

We note in passing that Eq. (59) can also be evaluated for finite temperature, assuming only $k_B T \ll E_F$. The result is (see Appendix B)

$$\Delta\sigma_{\mu\mu}^{\text{qcl}} \approx \frac{4\sigma_0}{ak_F \hbar\omega_c E_F} \times \sum_{\mathbf{g}} \frac{a\bar{g}_\mu^2}{2\pi g} |V_{\mathbf{g}}|^2 \left\{ \frac{1 - F_g}{2} + F_g \cos^2 \left(gR_c - \frac{\pi}{4} \right) \right\}, \quad (61)$$

where $\sigma_0 = e^2 N_s \hbar / (\Gamma_0 m)$, $F_g = F(gaT/2\pi T_a)$ with $F(x) = x/\sinh(x)$, and $k_B T_a = ak_F \hbar\omega_c / (2\pi)^2$ defines a critical temperature T_a above which the Weiss oscillations are washed out. Formulas of this type have been given by Beton *et al.*⁵⁹ As is well known,³⁶ the low-field SdH oscillations show a similar exponential temperature damping with a prefactor $F(T/T_c)$, where the critical temperature T_c is given by $k_B T_c = \hbar\omega_c / (2\pi^2)$. [Note that considerable overlap of only thermally broadened LL's sets in for $T \gtrsim 2T_c$ and that $F(T/T_c)$ reduces the amplitude of the oscillations by more than an order of magnitude for $T \gtrsim 5T_c$.] Since $T_a/T_c = ak_F/2 \gg 1$, the Weiss oscillations survive to considerably higher temperatures than the SdH oscillations. We see from Eq. (61) that, due to the factor F_g , the oscillatory contributions of higher harmonics (larger g) are increasingly smeared out with increasing temperature. Only for $gaT \ll 2\pi T_a$, i.e., for $\pi g R_c k_B T \ll E_F$, are the terms in Eq. (61) equivalent

to those of Eq. (60).

To make contact to previous work,^{8,15,20,41} we note that for the simple model (5) with $V_{xy} = 0$ the minima of the band conductivity occur if the flat band condition (1) is satisfied at the Fermi energy $E_F = \frac{1}{2}m\omega_c^2 R_c^2$, i.e., for $2R_c = a(\lambda - \frac{1}{4})$. The energetic distance between adjacent flat bands is estimated as $\Delta_\lambda = \partial E_F / \partial \lambda$, i.e., $\Delta_\lambda = E_F a / R_c = 2\pi^2 k_B T_a$. This energy determines the critical temperature T_a for the thermal damping of the Weiss oscillations, $T_a/T_c = \Delta_\lambda / \hbar\omega_c = k_F a / 2 \gg 1$. (In typical experiments^{1,20} with $a \approx 300$ nm and $N_s \approx 3 \times 10^{11}$ cm⁻² one has $ak_F \approx 41$.)

We want to emphasize the following important feature of the classical approximation: If the superlattice potential, Eq. (4), is additive in the sense that $V(x, y) = V_x(x) + V_y(y)$, i.e., if $V_{\mathbf{g}} = 0$ whenever $g_x g_y \neq 0$, then $\Delta\sigma_{yy}^{\text{qcl}}$ depends only on $V_x(x)$ and not on $V_y(y)$. Thus, if we start with the 1D modulation $V_x(x)$ and then add a modulation $V_y(y)$ in the other direction, the value of $\Delta\sigma_{yy}^{\text{qcl}}$ does not change. For sufficiently small collision broadening, this prediction of the classical approximation is neither in agreement with experimental results^{20,15} nor with the quantum-mechanical result.

2. Effect of subband splitting

If the collision broadening is so small that the modulation-induced subband splitting of the Landau levels is (partially) resolved, the quasiclassical approximation, neglecting the dependence of the spectral functions $A_{n,\alpha}(E)$ on the internal quantum numbers $\alpha = (\mathbf{k}, j)$, is not allowed. In order to calculate the band conductivity to lowest order in the modulation strength, one may still replace $[A_{n,j;\mathbf{k}}(E)]^2$ by $[A_n(E)]^2$. The product $A_{n,j;\mathbf{k}}(E)A_{n,j';\mathbf{k}}(E)$ for well-resolved subbands $j' \neq j$ is, however, much smaller, and may be neglected. As a consequence, the matrix elements $|(n, j'; \mathbf{k}| v_\mu |n, j; \mathbf{k})|^2$ are missing from the sum in Eq. (55), which thus has a smaller value than that corresponding to the complete trace (57) obtained in the quasiclassical limit. As a result, the full quantum-mechanical calculation yields a smaller value for the band conductivity than the quasiclassical approximation. For a fixed value of the magnetic field B ($p/q = 5$), this reduction has been demonstrated previously.^{20,60} In Fig. 7 we demonstrate the suppression of the band conductivity $\Delta\sigma_{yy}$ with increasing ratio V_y/V_x for the simple model (5) with $V_{xy} = 0$.⁵⁶ For $V_y = 0$, the matrix elements of $v_y^{(p)}$, Eq. (33), are diagonal in $x_0 = -l^2 k_y$, or, in the back-folded band-structure picture over the MBZ, in $\alpha = (\mathbf{k}, j)$, and the j, j' sum in Eq. (55) contains only diagonal elements $j' = j$. With increasing V_y , gaps open between the subbands (different j values) [cf. Figs. 3(a) and 3(d)], the eigenstates of the Hamiltonian matrix (24) rotate in the p -dimensional space, and off-diagonal matrix elements of $v_y^{(p)}$ arise. While $\text{tr}^{(p)} [v_y^{(p)}]^2$ is unchanged, the reduced weight of the off-diagonal ($j' \neq j$) matrix element due to the reduced overlap of the spectral functions, $A_{n,j;\mathbf{k}}(E)A_{n,j';\mathbf{k}}(E)$,

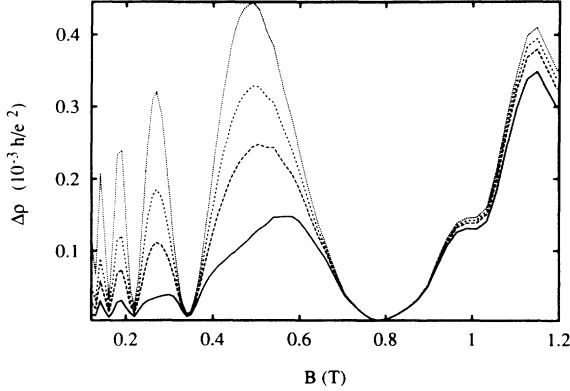


FIG. 7. Band resistivity $\Delta\rho_{xx}$ for $V(x,y) = V_x \cos Kx + V_y \cos Ky$ as a function of the magnetic field B for different values of V_y/V_x . From top to bottom: $V_y/V_x = 0.0, 0.5, 0.75, 1.0$. ($a \equiv 2\pi/K = 300$ nm, $V_x = 0.175$ meV, $\Gamma_0 = 0.015\sqrt{B}$ [T] meV, $N_s = 3 \times 10^{11}$ cm $^{-2}$, $T = 4.65$ K.)

leads to a suppression of $\Delta\sigma_{yy}$ with increasing V_y . The parameters in Fig. 7 are chosen such that, at $B = 0.5$ T, the total width of the Landau band at the Fermi level is $W_F \approx 0.3$ meV, and the flux ratio (2) is $\Phi/\Phi_0 \approx 11$. Then, according to Fig. 2 for $q/p \approx 0.1$, the subbands group into about ten clusters, most of which are well resolved for the chosen collision broadening $\Gamma_0 \approx 0.01$ meV.

Due to thermal broadening ($T = 4.65$ K), the Shubnikov-de Haas (SdH) oscillations are not resolved in Fig. 7. (For $B > 0.8$ T, SdH oscillations begin to occur leading to structured line shapes.) Therefore, the oscillatory structure of $\Delta\rho_{xx} \propto \Delta\sigma_{yy}$ (see below) as a function of the magnetic field reflects the Weiss oscillations² which show minima in the band conductivity whenever the cyclotron radius of electrons at the Fermi surface satisfies the commensurability equation (1).

C. Scattering conductivity

A nonzero band conductivity related to the guiding center drift occurs only in modulated systems. This conduction mechanism adds to the usual conduction mechanism in quantizing magnetic fields, i.e., the scattering of electrons between adjacent Landau levels owing to the impurity potentials. The contribution of this impurity scattering to the conductivity is determined by the overlap $A_{n;\alpha}(E)A_{n+1;\alpha'}(E)$ of the spectral functions of adjacent LL's, which vanishes in the absence of impurities (within the framework of negligible LL mixing by the modulation potential).

1. Consistent theory

Besides its main peak at $E \approx \varepsilon_{n\alpha}$, the spectral function

$$A_{n\alpha}(E) = \frac{1}{\pi} \frac{\text{Im}\Sigma^-(E)}{[E - \varepsilon_{n\alpha} - \text{Re}\Sigma^-(E)]^2 + [\text{Im}\Sigma^-(E)]^2} \quad (62)$$

has satellite maxima near the band centers of the other LL's ($n' \neq n$), as we have emphasized below Eq. (41). Assuming the level broadening due to both the modulation potential and the impurity scattering to be small compared to the cyclotron energy, $|\varepsilon_{n\alpha} + \Sigma^-(E) - \hbar\omega_c(n + \frac{1}{2})| \ll \hbar\omega_c$ for all n , one obtains for $E \approx \varepsilon_{n\alpha}$ from Eqs. (40) and (41),

$$A_{n\pm 1,\alpha'} \approx \frac{1}{\pi} \frac{\text{Im}\Sigma^-(E)}{(\hbar\omega_c)^2} \approx \frac{2}{\pi} \left(\frac{\pi l \Gamma_0}{\hbar\omega_c} \right)^2 D_n(E), \quad (63)$$

where the last step is consistent with our leading-order approximation.

The inter-LL ($n' \neq n$) contributions to the conductivity formula (55) are dominated by the zeroth-order velocity matrix elements given in Eq. (31), which yield (after rearranging the sum)

$$\sigma_{\mu\mu}^{\text{sc}}(E) = \frac{e^2 \hbar l^2 \omega_c^2}{2\pi} \sum_{nj} \left(2(n+1) \int d^2k A_{n;\alpha}(E) A_{n+1;\alpha}(E) \right). \quad (64)$$

In the energy range of the LL with number \tilde{n} , i.e., for $|E - \hbar\omega_c(\tilde{n} + \frac{1}{2})| \ll \hbar\omega_c$, only the terms with $n = \tilde{n}$ and $n+1 = \tilde{n}$ contribute considerably to the n sum in Eq. (64). Then, one finds from Eq. (63) together with Eq. (40)

$$\sigma_{\mu\mu}^{\text{sc}}(E) = \frac{e^2}{\hbar} \sum_n (2n+1) [2\pi l^2 \Gamma_0 D_n(E)]^2. \quad (65)$$

The same analytical form has been derived for the homogeneous 2D ES.³⁶ In Eq. (65), however, $D_n(E)$ is the contribution of the n th LL to the DOS of the modulated 2D ES, which reflects the n -dependent oscillatory width of the modulation-induced Landau bands. Thus, Eq. (65) describes amplitude-modulated SdH oscillations with maximum peak height for minimum bandwidth. For the simple model (5) with $V_{xy} = 0$, the maximum peak heights occur if the flat band condition, Eq. (1) with $R_c = R_n$, is satisfied. Note that under this condition the guiding-center drift velocity vanishes and the band conductivity becomes minimum. Similar to the Weiss oscillations of the band conductivity, the amplitude oscillations of the scattering conductivity (65) survive to higher temperatures ($k_B T \gtrsim \hbar\omega_c$) where the individual SdH oscillations are smeared out. Inserting Eq. (65) into Eq. (54), one obtains (for $k_B T$ much larger than the total width of the Landau bands)

$$\sigma_{\mu\mu}^{\text{sc}} = \frac{e^2}{2\pi\hbar} \sum_n [-f'(E_n)] (2n+1) \tilde{\Gamma}_n. \quad (66)$$

Here

$$\tilde{\Gamma}_n = 2\pi \int dE [2\pi l^2 \Gamma_0 D_n(E)]^2 \quad (67)$$

defines an effective scattering rate $\tau_n^{-1} = \tilde{\Gamma}_n/\hbar$. Whereas the integral over $D_n(E)$ itself is normalized and indepen-

dent of n , $\tilde{\Gamma}_n$, being an integral over the square of $D_n(E)$, oscillates as a function of n . It becomes small for broad Landau bands and large for narrow ones, with the value for the unmodulated system as an upper limit.

For the general case, a further analytical evaluation of the oscillatory behavior of the scattering conductivity seems hardly possible, since the origin of these oscillations is hidden in the width of the $D_n(E)$ peaks, i.e., ultimately in the quantum-mechanical energy spectrum. This was much easier in the quasiclassical limit of the band conductivity, where the oscillations were dominated by those of the velocity-matrix elements, and the modulation effect on the energy eigenvalues could be neglected.

For our simple model (5) with $V_{xy} = 0$ we know that $\tilde{\Gamma}_n$, Eq. (67), has maxima for flat bands. For $T_c \ll T \ll T_a$, the n sum in Eq. (67) is easily evaluated, and with $n_F = E_F/\hbar\omega_c$ and $E_F = \hbar^2 N_s \pi/m$ one obtains the Drude-type result

$$\sigma_{\mu\mu}^{\text{sc}} = (e^2 N_s / m \omega_c^2) \tau_{n_F}^{-1}. \quad (68)$$

These considerations demonstrate clearly that the Weiss oscillations of the scattering conductivity result from quantum oscillations of the transport scattering rate. They also explain that, at a given temperature, these oscillations can be observed down to much lower magnetic fields than the modulation-induced oscillations of the magnetocapacitance.^{19,13,61} The latter result from amplitude oscillations of the contributions $D_n(E)$ of individual LL's to the DOS and disappear when these are not resolved.

A numerical comparison of band and scattering conductivity is given in Sec. V below.

2. Deficiencies of inconsistent approach

To obtain the leading-order modulation-induced oscillations of the scattering conductivity in terms of the scattering rate, Eq. (67), it was essential to evaluate the Kubo formulas with the correct spectral functions, i.e., the spectral functions obtained from the SCBA-type approximation (38) of the self-energy which satisfies the self-consistency requirements (47) and (48). These spectral functions have satellite peaks at adjacent LL's, so that the overlap of spectral functions belonging to adjacent LL's leads, according to Eqs. (41) and (63), to the square of the partial DOS in Eq. (65). Mathematically, this property of the spectral function is hidden in the energy dependence of the self-energy. If we neglect this energy dependence and *ad hoc* replace the self-energy with a constant,

$$\Sigma^-(E) \rightarrow \Sigma_L^- = \Delta_L - \frac{i}{2} \Gamma_L, \quad (69)$$

the spectral function (62) reduces to a simple Lorentzian, and instead of Eq. (63) we obtain $A_{n\pm 1, \alpha'} \approx \Gamma_L / [2\pi(\hbar\omega_c)^2]$. Then, one of the factors $D_n(E)$ in Eq. (65) has to be replaced with $\Gamma_L / (2\pi l \Gamma_0)^2$, and one obtains

$$\sigma_{\mu\mu}^0(E) = \frac{e^2}{\hbar} l^2 \Gamma_L \sum_L (2n+1) D_n(E). \quad (70)$$

Furthermore, if $k_B T$ is much larger than the total width of the Landau bands, one obtains now Eq. (66) with the n -independent scattering rate

$$\tilde{\Gamma}_n^0 = 2\pi l^2 \int dE \Gamma_L D_n(E) = \Gamma_L, \quad (71)$$

since the number of states is the same in all Landau bands, independently of their width. Thus, with the inconsistent approximation (69) one loses the leading-order oscillations of scattering rate and scattering conductivity. For lower temperatures, one may insert Eq. (70) directly into Eq. (54). If one neglects collision broadening, one has, assuming Eq. (2) to hold,

$$D_n^0(E) = \sum_{j=1}^p \int_{\text{MBZ}} \frac{d^2 k}{(2\pi)^2} \delta[E - E_{n,j}^{(p)}(\mathbf{k})], \quad (72)$$

which reduces for a 1D superlattice in the x direction [$E_{n,j}^{(p)} = \hbar\omega_c(n + \frac{1}{2}) + \tilde{E}_{n,j}^{(p)} \rightarrow E_{n, k_y + 2\pi j/a_y}$] to

$$D_n^0(E) = \frac{1}{2\pi a_x} \int_0^{a_x/l^2} dk_y \delta(E - E_{n, k_y}). \quad (73)$$

With this form of $D_n(E)$ in Eq. (70), the result is

$$\sigma_{\mu\mu}^0 = \frac{e^2 l^2 \Gamma_L}{h a_x} \int_0^{a_x/l^2} dk_y \sum_n (2n+1) [-f'(E_{n, k_y})]. \quad (74)$$

Exactly this formula has been obtained by Vasilopoulos and Peeters,⁶ who also tried to explain the Weiss oscillations of the scattering conductivity [in their paper $\Gamma_L = N_l U_0^2 / (\pi l^2 \Gamma)$]. They did not evaluate the Kubo formula directly, but started with a "quantum Boltzmann equation," which does not include collision broadening of the spectral functions in a consistent manner. Their result, however, is not in agreement with characteristic features of the experiments.^{19,13,61} First, it cannot explain why the Weiss oscillations of the scattering conductivity can be resolved down to much smaller B values than the Weiss-type oscillations of the DOS (magnetocapacitance). Since Eq. (74) can be obtained from Eq. (65) by replacing one $D_n(E)$ factor with an n -independent term, it predicts the same type of oscillations for scattering conductivity and DOS. Second, these oscillations are much smaller (more than two orders of magnitude)⁶ than those of the band conductivity, in disagreement with the experiments. From a systematic point of view, the problem with Eq. (74) is that it omits the leading-order oscillations (see above), but includes terms of second order in the small ratio of modulation potential over cyclotron energy. The same holds for the correction terms introduced later by Refs. 17 and 40, which correspond in our formulation to modulation-dependent higher-order corrections to the zeroth-order inter-LL ($n \neq n'$) velocity matrix elements (31). If one wants to include such higher-order effects in the conductivity, one should for consistency reasons calculate the energy spectrum also to higher order and include LL mixing due to the superlattice potential.

In conclusion, we want to emphasize that for a correct

understanding of the Weiss oscillations of the scattering conductivity a consistent inclusion of collision broadening effects in the transport calculation is inevitable. In our SCBA-type approach this leads to the result that, at zero temperature, the conductivity is proportional to the square of the DOS (of the actual 2D ES in the presence of both the superlattice and the disorder) at the Fermi energy, as it should be for elastic scattering.³⁶ The results obtained with the inconsistent approach used by Vasilopoulos and Peeters^{6,17} underestimate the oscillatory effects. This critique applies also to the recent work of Xue and Xiao,⁶² who adapted this approach to the case of a magnetically modulated 2D ES.

D. Hall conductivity

The 2D ES in a 2D lateral superlattice has been discussed in connection with the quantized Hall effect.^{34,35,52} If, at zero temperature, the Fermi energy falls into a gap of the Hofstadter-type energy spectrum (say for $\Phi/\Phi_0 = p/q$), then the (spin-degenerate) Hall conductivity has a quantized value $\sigma_{yx} = r(2e^2/h)$, with an integer r . For large values of p and q , large positive and negative values of r are possible. The net change of σ_{yx} , obtained while sweeping E_F across a whole Landau band, is $2e^2/h$. We now briefly discuss the relation between these results and the physical situation of our present interest.

1. Absence of disorder

In the absence of disorder, one can evaluate Eq. (56) with the exact eigenstates (12) and the exact energy eigenvalues $E_\beta(\mathbf{k})$ satisfying

$$[H(\mathbf{k}) - E_\beta(\mathbf{k})] u_{\mathbf{k}}^{(\beta)}(x, y) = 0. \quad (75)$$

For a weak periodic potential perturbing the Landau quantized 2D ES, the quantum numbers $\beta = (n, j)$ can be chosen as a LL quantum number n and a subband index j , although the eigenstates $\Psi_{\mathbf{k}}^{(\beta)}$, Eq. (12), are superpositions of the states (21) with different n and κ values. For zero temperature ($T \rightarrow 0$) and E_F in a gap, Eq. (56) reduces to a sum over occupied subbands, $\sigma_{yx} = \sum_{\beta}^{\text{occ}} \sigma_{yx}^{\beta}$, with the contribution of subband β given by

$$\sigma_{yx}^{\beta} = -\frac{e^2 \hbar}{\pi^2} \int d^2 k \text{Im} \sum_{\beta'} \frac{\langle \beta, \mathbf{k} | v_x | \beta', \mathbf{k} \rangle \langle \beta', \mathbf{k} | v_y | \beta, \mathbf{k} \rangle}{[E_\beta(\mathbf{k}) - i0^+ - E_{\beta'}(\mathbf{k})]^2}. \quad (76)$$

Note that the diagonal matrix elements ($\beta' = \beta$) are real and do not contribute to the sum. Taking the derivatives of Eq. (75) with respect to k_x and k_y , and using Eq. (14), one obtains

$$\sigma_{yx}^{\beta} = \frac{e^2}{\pi^2 \hbar} \int d^2 k \text{Im} \left\langle \frac{\partial u_{\mathbf{k}}^{\beta}}{\partial k_y} \middle| \frac{\partial u_{\mathbf{k}}^{\beta}}{\partial k_x} \right\rangle. \quad (77)$$

Here the completeness of the states $\Psi_{\mathbf{k}}^{(\beta')}$ in the subspace of states with fixed \mathbf{k} was exploited, as well as the fact

that the contribution of $\beta' = \beta$ is zero.

From the form (77) it has been recognized that the Hall conductivity is related to a topological invariant on a torus (the MBZ with periodic boundary conditions), which is the mathematical reason for the quantization.^{43,63} For the explicit evaluation of Eq. (77), one may express the integrand as the curl (in \mathbf{k} space) of the vector with the components $a_{\mu}^{\beta}(\mathbf{k}) = \langle u_{\mathbf{k}}^{\beta} | \partial u_{\mathbf{k}}^{\beta} / \partial k_{\mu} \rangle$, and apply Stoke's theorem to obtain a contour integral along the boundary of the MBZ. The quantized result is non-trivial owing to the (phase) singularities of $u_{\mathbf{k}}^{\beta}$ considered as a function of \mathbf{k} in the MBZ.^{43,31}

In view of our decomposition of conductivities into intra-LL ("band") and inter-LL ("scattering") contributions, the following procedure due to Usov³¹ is illuminating. Note that the scalar product in Eq. (77) involves the 2D integral of wave functions over real space. In our lowest-order perturbative treatment of the superlattice potential, this can be reduced to the simpler scalar product in the p -dimensional space. Since the discretely quantized values cannot change if we change the amplitude of the modulation potential continuously (while closing no gaps), we may replace the exact eigenstates $\Psi_{\mathbf{k}}^{(\beta)}$, with $\beta = (n, j)$, by the approximate ones, Eq. (23). Then

$$u_{\mathbf{k}}^{\beta}(\mathbf{r}) = \sum_{\kappa=1}^p u_{\kappa}(\mathbf{k}; j, n) f_{\mathbf{k}}^{n, \kappa}(\mathbf{r}), \quad (78)$$

with

$$f_{\mathbf{k}}^{n, \kappa}(\mathbf{r}) = e^{-i\mathbf{k} \cdot \mathbf{r}} \langle \mathbf{r} | n, \kappa; \mathbf{k} \rangle \quad (79)$$

determined by the basis states (21). Inserting Eq. (78) into Eq. (77), we obtain derivatives of the $f_{\mathbf{k}}^{n, \kappa}$, which can be evaluated using Eq. (21) and the properties of the Landau functions (6), i.e., of the Hermite polynomials. Due to the orthogonality and normalization of the basis functions (21), the contributions of the $f_{\mathbf{k}}^{n, \kappa}$ can be evaluated explicitly, with the result

$$\sigma_{yx}^{\beta} = \frac{e^2}{\pi^2 \hbar} \int d^2 k \text{Im} \left[\frac{i}{2} l^2 + \sum_{\kappa=1}^p \frac{\partial u_{\kappa}^*}{\partial k_y} \frac{\partial u_{\kappa}}{\partial k_x} \right], \quad (80)$$

where the arguments $(\mathbf{k}; j, n)$ of the u_{κ} have been suppressed. The first term in the square brackets is immediately evaluated to yield

$$\sigma_{yx}^{\beta, 0} = \frac{2e^2}{h} \frac{1}{p}. \quad (81)$$

This is just the contribution of one out of p spin-degenerate subbands to the free-electron Hall conductivity

$$\sigma_{yx}^0 = \nu e^2 / h = e^2 N_s / m \omega_c, \quad (82)$$

with $\nu = 2\pi l^2 N_s$ the filling factor. Apparently this result follows directly from Eq. (56) if we neglect the superlattice modulation and use the zeroth-order velocity matrix elements (31), leading to inter-LL contributions only.

The remaining term $\Delta \sigma_{yx}^{\beta} = \sigma_{yx}^{\beta} - \sigma_{yx}^{\beta, 0}$ in Eq. (80) is the intra-LL contribution. It can be obtained directly from the $n' = n$ terms of the sum in Eq. (56), using the

eigenvectors $u^{(p)}(\mathbf{k}; j, n)$ and the eigenvalues $\tilde{E}_{n,j}^{(p)}(\mathbf{k})$ of the $p \times p$ Hamiltonian matrix (24), and the representation (33) for the velocity components. This contribution can be written as a contour integral along the boundary of the MBZ of the vector

$$\mathbf{a}(\mathbf{k}; j, n) = \sum_{\kappa=1}^p u_{\kappa}^* \frac{\partial u_{\kappa}}{\partial \mathbf{k}} = i \sum_{\kappa=1}^p |u_{\kappa}|^2 \frac{\partial \varphi_{\kappa}}{\partial \mathbf{k}}, \quad (83)$$

where the notation $u_{\kappa} = |u_{\kappa}| \exp(i\varphi_{\kappa})$ is used. As shown by Usov,³¹ this ‘‘band’’ contribution can be written as

$$\Delta_{yx}^{\beta} = \frac{2e^2}{h} \frac{q}{p} S^{\beta}, \quad (84)$$

where the integer S^{β} is the sum of the winding numbers of the phase (of a representative component u_{κ}) around the singularities contained in the (p/q) -fold of the MBZ. These integers have the properties that $qS^{\beta} + 1 = rp$ is an integer multiple of p , and that the sum over all the S^{β} belonging to the same LL vanishes, $\sum_{j=1}^p S^{(j,n)} = 0$. For the simple model (5) and a flux ratio $\Phi/\Phi_0 = p/q$ with $p = 2$, it is easy to evaluate the contour integral around the MBZ explicitly. With the notation of Eqs. (28) and (29), we obtain ($p = 2, q$ odd)

$$S^{(j,n)} = (-1)^j \text{sgn} \left[(-1)^{(q-1)/2} \tilde{V}_x \tilde{V}_y \tilde{V}_{xy} \right], \quad (85)$$

provided $\tilde{V}_x \tilde{V}_y \tilde{V}_{xy} \neq 0$, and the two subbands ($j = 1, 2$) are separated by a gap. Note that for the Hofstadter case, $V_{xy} = 0$, the gap (for $p = 2$) closes, and Usov’s formalism is not applicable.

The quantized values of the Hall conductivity are obtained if the Fermi energy falls into a gap of the energy spectrum. It seems reasonable to assume that σ_{yx} interpolates smoothly between the adjacent quantized values as E_F is swept through a subband.

It has been argued⁵³ that weak disorder does not destroy the quantization if it does not smear out the corresponding gap.

2. Effect of disorder and temperature

We now include the effect of disorder within the simple, but consistent treatment of collision broadening discussed in Sec. IV A.

We first consider the quasiclassical limit of large collision broadening, where the effect of the superlattice potential on the energy spectrum, i.e., on the spectral and the Green’s function in Eq. (56), can be neglected.

The analog of the band conductivity is the intra-LL ($n' = n$) contribution $\Delta\sigma_{yx}$. Following the procedure of Appendix A, we can evaluate, in the quasiclassical limit, the sum over the internal quantum numbers exactly,

$$\begin{aligned} & \int d^2k \sum_{j,j'} ((n, \alpha || v_x || n, \alpha')) ((n, \alpha' || v_y || n, \alpha)) \\ &= \int d^2k \text{tr}^{(p)} \left[v_x^{(p)}(\mathbf{k}; n) v_y^{(p)}(\mathbf{k}; n) \right] \\ &= -2\pi \left(\frac{l}{\hbar} \right)^2 \sum_{\mathbf{g}} g_x g_y \left| \tilde{V}_n(\mathbf{g}) \right|^2. \end{aligned} \quad (86)$$

Since this expression is real, one can evaluate the imaginary part in Eq. (56), obtaining

$$\text{Im} [A_n(E) dG_n^-(E)/dE] = (\pi/2) d[A_n(E)]^2/dE.$$

Integrating by parts introduces the derivative of the Fermi function, and Eqs. (54) and (58)–(61) for the diagonal conductivity $\Delta\sigma_{\mu\mu}$ hold also for $\Delta\sigma_{yx}$ if one replaces $|\tilde{g}_{\mu}|^2$ by $-g_x g_y$. For model potentials (5) with a reflection symmetry, e.g., $V(-x, y) = V(x, y)$ or $V(x, -y) = V(x, y)$, the intra-LL contribution to the Hall conductivity vanishes in the quasiclassical limit,

$$\Delta\sigma_{yx}^{\text{qcl}} = \Delta\sigma_{xy}^{\text{qcl}} = 0. \quad (87)$$

Thus, in the quasiclassical limit, there is no ‘‘band-conductivity’’ contribution to the Hall conductivity.

The inter-LL contribution to the Hall conductivity (56) is dominated by the zeroth-order velocity matrix elements (31). In the quasiclassical limit, these lead to the Hall conductivity of an unmodulated 2D ES, showing at sufficiently low temperature SdH oscillations superimposed on the free-electron Drude result, but no Weiss oscillations.^{54,36} Modulation-induced oscillations can arise only in higher orders of the small ratio of modulation potential over cyclotron energy. Such terms have to be neglected in our leading-order perturbation theory, which neglects the coupling of LL’s by the superlattice potential.

In the quasiclassical limit we assumed that all effects of the (weak) superlattice potential on the energy spectrum are smeared out by the (large) collision broadening, and obtained as a leading-order result for the Hall conductivity the classical Drude result. The same arguments hold for the inter-LL contribution to σ_{yx} if the collision broadening of the LL’s is of comparable magnitude to or even smaller than the modulation-induced bandwidth, but both are much smaller than $\hbar\omega_c$. Then, the leading-order inter-LL contribution is just the classical Drude term (82). There is no analog of the mechanism which leads to the Weiss oscillations of the scattering conductivity. According to Eq. (31), the matrix elements of v_x are imaginary, and those of v_y are real, so that $\text{Re} dG_{n',\alpha'}^-/dE$ enters Eq. (56). For $E \approx E_{n,\alpha}$ one has to leading order $\text{Re} dG_{n\pm 1,\alpha'}^-/dE \approx -(\hbar\omega_c)^{-2}$, instead of the corresponding Eq. (63) for $\sigma_{\mu\mu}^{\text{sc}}$. Whereas for $k_B T \gg \hbar\omega_c$ the E integral in Eq. (55) for the diagonal components of the conductivity tensor leads to Eq. (67), the E integral in Eq. (56) does not lead to an oscillatory n dependence, since the integrand contains only the first power of the normalized factor $D_n(E)$, but not its square as in the case of the diagonal scattering conductivity.

Finally we comment on the intra-LL contribution $\Delta\sigma_{yx}$ for small collision broadening, where the subband structure is partially resolved. For $T \rightarrow 0$, one expects a result $\Delta\sigma_{yx}(E_F)$ intermediate between the zero value in the quasiclassical limit and the fluctuating result in the absence of disorder, with quantized values in the energy gaps. In the absence of disorder, all the subband contributions to $\Delta\sigma_{yx}$ from a given LL add up to zero. Thus, the thermal average of $\Delta\sigma_{yx}$ for each Landau level will

also be zero if $k_B T$ is larger than the modulation-induced width of a Landau band, and certainly for $k_B T \gg \hbar \omega_c$.

In summary, in our leading-order approximation we have to replace the Hall conductivity with the classical Drude result (82). For $\omega_c \tau \gg 1$, i.e., to leading order in the collision broadening, we then obtain for the resistivity tensor

$$\rho_{xx} = \frac{\sigma_{yy}}{(\sigma_{yx}^0)^2}, \quad \rho_{yy} = \frac{\sigma_{xx}}{(\sigma_{yx}^0)^2}, \quad \rho_{yx} = \frac{1}{\sigma_{yx}^0}. \quad (88)$$

V. SUMMARY AND DISCUSSION

We have generalized the self-consistent magnetotransport theory previously developed for two-dimensional electron systems with a periodic modulation in one lateral direction⁸ to the case of 2D ES's with a weak 2D lateral superlattice potential. The theory includes the correct energy spectrum, which is determined by two different types of commensurability effects. The internal subband splitting of the Landau bands reflects the commensurability of the lattice constant a and the magnetic length l , expressed in terms of the flux ratio (2). The total width of a Landau band is determined by the ratio of a and the cyclotron radius $R_n = l\sqrt{2n+1}$ of this Landau band. For a simple cosine potential on a square lattice (the Hofstadter case), this width oscillates as a function of n and becomes minimum, if Eq. (1) holds with $R_c = R_n$. This oscillation of the Landau bandwidth is the origin of the observed Weiss oscillations of the resistivity components, which are periodic in B^{-1} . The resistivity is governed by two additive contributions to the conductivity, which are of different origins and have different properties. The first, called "band conductivity," is closely related to the classical guiding-center drift of cyclotron orbits in the periodic electric field of the superlattice. It is proportional to the square of the group velocity of the modulation-induced Landau bands. It becomes minimum if flat bands are located at the Fermi energy, i.e., if Eq. (1) holds, and it vanishes identically for the unmodulated, homogeneous 2D ES. The second contribution, called "scattering conductivity," reflects the properties of the scattering rate owing to the scattering of electrons by randomly distributed impurities. It is determined by the thermal average of the squared density of states, and becomes maximum if flat bands are located at the Fermi level, i.e., if Eq. (1) holds. Thus, both the band conductivity and the scattering conductivity oscillate as a function of B^{-1} with the same period given by Eq. (1), but with opposite phases. In both cases the Weiss oscillations survive at elevated temperatures, where the SdH oscillations are already smeared out. All this has been nicely verified in experiments on samples with a 1D modulation, where both the band conductivity and the scattering conductivity can be observed separately on the same sample.^{1,61}

To obtain the correct leading-order oscillations of the scattering conductivity, it was important to treat the collision broadening of the Landau levels and the transport coefficients in a consistent manner.

The relative magnitude of band conductivity and scattering conductivity depends sensitively on the relative magnitude of the superlattice potential and the collision broadening. If the collision broadening is so large that the internal subband structure of the LL's (see Fig. 2) is not resolved, we obtain for the 2D superlattice essentially the same result as for the 1D superlattice with the same period. Then the band conductivity is given by the quasiclassical approximation, Eqs. (58)–(61), being proportional to the square of the modulation amplitude and inversely proportional to the collision broadening Γ_0 ($\propto \tau^{-1}$). The scattering conductivity in this situation is, according to Eqs. (66) and (67), on the average (i.e., apart from the modulation-induced oscillations) proportional to Γ_0 , in agreement with the classical Drude result. If, however, the collision broadening is so small that the internal structure is, at least partially, resolved, then our theory predicts a drastic suppression of the band conductivity by the 2D superlattice below the value obtained for the corresponding 1D superlattice. This is demonstrated in Fig. 7, and also, for a fixed value of the magnetic field and variable Fermi energy, in Ref. 20.⁶⁰ We believe that the dramatic suppression of the band conductivity observed on holographically structured samples at elevated temperatures ($T \sim 4$ K) is correctly described by this mechanism. The resolved subband splitting tends to enhance the scattering conductivity, as is easily understood from Eq. (67).

At low temperatures the Weiss oscillations occur as amplitude modulation of the resolved SdH peaks.¹⁶ In this situation the dependence of the conductivity contributions on collision broadening and superlattice potential is very complicated. Whereas the scattering conductivity decreases on the average with decreasing collision broadening, particularly narrow Landau bands (or subbands) may lead to particularly high peaks, thus opposing the general trend. For the band conductivity, on the other hand, decreasing collision broadening ($\sim \Gamma_0$) means on the average less overlap of different subbands (or clusters of subbands), and therefore an overall reduction. The peak due to a well-resolved subband (or cluster) will, however, increase inversely proportional to Γ_0 , similar to the case when no subbands are resolved.

In Fig. 8 we show, for two different situations, the calculated band and scattering contributions together with the resulting total resistivity, according to Eq. (88). From the classical formula (61) (with $V_g = 0$ for $g > 2\pi/a$) one would expect the band conductivity to be proportional to V_x^2/Γ_0 . Then the band conductivity in Fig. 8(a) should be larger than that in Fig. 8(b) by a factor of ≈ 3 . This is roughly true near $B = 0.54$ T (LL $n = 11$) and near $B = 0.37$ T (thermally overlapping LL's $n = 16$ and 17), but certainly not near $B = 0.96$ T (LL $n = 6$), where the factor is only 1.3.

From Fig. 2 we understand that the situation must be much more complicated than predicted by the quasiclassical approximation. According to Eq. (9), the effective bandwidth at the Fermi level is $W_F \approx 4V_x(\pi^2 R_c/a)^{-1/2}$. For $B = 0.96$ T (0.37 T) this means $W_F \approx 0.4$ meV (0.25 meV) for Fig. 8(a) and $W_F \approx 0.28$ meV (0.175 meV) for Fig. 8(b). The collision broadening at $B = 0.96$ T

(0.37 T) is $\Gamma_0 \approx 0.01$ meV (0.006 meV) for Fig. 8(a) and $\Gamma_0 \approx 0.015$ meV (0.009 meV) for Fig. 8(b). This is so small that in all cases the band conductivity is considerably reduced below its quasiclassical value due to subbands with nonoverlapping spectral functions.

From Fig. 2 we also understand that this quantum suppression of the band conductivity at $B = 0.96$ T should be more important in Fig. 8(a) than in Fig. 8(b). The flux ratio (2) at $B = 0.96$ T is $\Phi/\Phi_0 \approx 5.2$, and we see from Fig. 2 that for $q/p \approx 0.19$ the subbands are grouped into five clusters. The two outermost clusters are narrow and well separated from the three inner clusters. The widths of these inner clusters ($\sim 0.1W_F$) are comparable to each other, and to the width of the gaps between them. In the situation of Fig. 8(a) the overlap of spectral functions belonging to different inner clusters is safely negligible ($0.1W_F/\Gamma_0 \approx 4$), but not in the situation

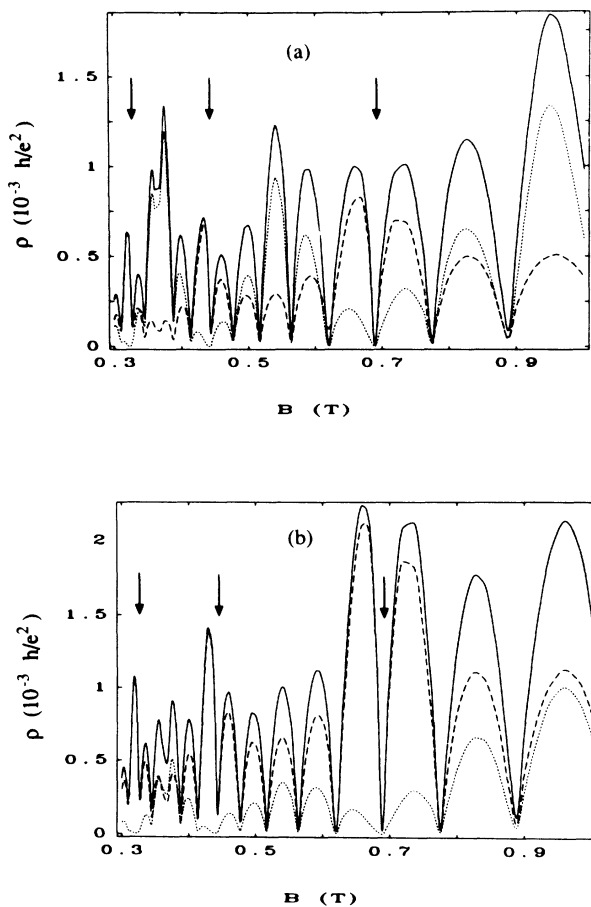


FIG. 8. Calculated resistivity ρ_{xx} for a 2DEG of mean density $N_s = 3 \times 10^{11} \text{ cm}^{-2}$ at temperature 1 K in a square superlattice of period $a = 150$ nm. Arrows indicate flat band positions. For (a) a collision broadening $\Gamma_0 = 0.010\sqrt{B}$ [T] meV and a potential strength $V_x = V_y = 0.250$ meV the total resistivity (solid lines) is dominated by the band resistivity (dotted lines), and (b) a collision broadening $\Gamma_0 = 0.015\sqrt{B}$ [T] meV and a potential strength $V_x = V_y = 0.175$ meV the total resistivity is dominated by the scattering resistivity (dashed lines).

of Fig. 8(b) ($0.1W_F/\Gamma_0 \approx 2$).⁵⁶

At $B = 0.37$ T, on the other hand, we see no such qualitative difference between the situation of Fig. 8(a) and that of Fig. 8(b). The flux ratio is $\Phi/\Phi_0 \approx 2.02$, and at $q/p \approx 0.495$ the subbands in Fig. 2 are grouped into two well-separated clusters in both situations.

We see from Fig. 8 that the suppression of the band conductivity, owing to better resolution of the subband structure as a consequence of smaller collision broadening, may be magnetic field dependent, with a stronger suppression below the quasiclassical value at higher magnetic fields. This is in agreement with recent experiments,¹⁶ in which the band conductivity was found to dominate the Weiss oscillations at low magnetic fields and to be suppressed at high magnetic fields.

The important message of Fig. 8 is the following. For high-mobility samples ($\mu \gtrsim 10^6 \text{ cm}^{-2}/\text{Vs}$) with a 2D superlattice ($a \sim 150$ nm) there exists a regime of modulation strengths, where the band conductivity is so suppressed below its quasiclassical (1D) value that it is of the same order of magnitude as the scattering conductivity. In this regime, tuning of the superlattice potential can lead from a situation like that in Fig. 8(a) to a situation like that in Fig. 8(b). In the former, the total resistivity is dominated by the band conductivity, with minima of the envelope function if the flat band condition (1) holds. In the latter, the resistivity is governed by the scattering conductivity, with maxima if Eq. (1) is satisfied. Exactly these band-conductivity dominated and scattering-conductivity dominated situations have recently been observed on high-mobility samples with nanostructured gates which allowed tuning of the modulation strength.¹⁶

In Fig. 8 the temperature ($T = 1$ K) was chosen such that each individual Landau band is resolved, but not, however, its internal subband structure. The result looks very similar to the experimental data¹⁶ obtained at a much lower temperature, $T \approx 50$ mK, i.e., $k_B T \approx 5 \mu\text{eV}$. Naively, one should expect the subband structure to be resolved at these low temperatures, but this is not seen in the experiment. This can be attributed to spatial fluctuations of the conduction-band edge. In order to resolve in a transport measurement a gap at the Fermi level of a width of several μeV , the fluctuation of the conduction-band edge due to electrostatic fields (e.g., due to fluctuations of the charged-donor distribution in the Si-doped $\text{Al}_x\text{Ga}_{1-x}\text{As}$ behind the spacer) must be smaller than a few μeV over the entire sample. This seems unrealistic. Taking an average over long-range ($\gg a, \lambda_{\text{free}}$) mesoscopic fluctuations has a similar effect to taking a thermal average. From the experiment¹⁶ we estimate for such fluctuations a distribution with an energetic width of about 0.1 meV.

Finally we want to comment on some basic assumptions made in our approach. In the experiments, the superlattice potential is created at some distance from the 2D ES, either by a nanostructured metal gate or by a holographic modulation of the charged-donor distribution behind the spacer. According to Poisson's law, the Fourier coefficients of this potential decay exponentially towards the 2D ES, so that higher Fourier coeffi-

icients die out more rapidly than the simple cosine potential of the fundamental periodicity. Moreover, the superlattice potential is screened by the 2D ES itself. The resulting screened potential should be the input of our model.^{4,8,12} Within the Thomas-Fermi approach, the screening length is determined by the thermodynamic density of states. If the temperature is so high that the individual Shubnikov-de Haas oscillations are not resolved in the transport coefficients, then, according to both the theory and the experiments,¹³ the thermodynamic DOS and, thus, the screening is independent of the magnetic field. In this situation our assumption of a fixed, B -independent superlattice potential is well justified. If the superlattice potential is created by a (close to harmonic) modulation of the charged-donor distribution or by a structured gate at a sufficiently large distance ($\gtrsim a$) from the 2D ES, our assumption of a weak, purely harmonic superlattice potential as in Eq. (5) with $V_{xy} = 0$ is also reasonable.

The inclusion of higher Fourier coefficients of the superlattice potential has been discussed in the analytical part of this paper. It modifies the single-particle spectrum, but qualitatively the Hofstadter-type subband splitting of the Landau bands will last; cf. Figs. 4 and 5. As a consequence, the mechanism for the suppression of the band conductivity will remain qualitatively unchanged. On the other hand, the additional Laguerre factors with different (incommensurate) arguments will destroy the exact periodicity of the conductivities in B^{-1} , and both the maxima and the minima of the oscillations will become less pronounced.¹²

The extension of our theory to stronger superlattice potentials ($V_x \sim V_y \gtrsim \hbar\omega_c$) requires more numerical effort. Then, the lowest-order perturbation treatment is no longer adequate, and the mixing of different Landau levels by the superlattice potential must be taken into account. This immediately leads to much larger dimensions of the Hamiltonian matrix to be diagonalized. Nevertheless, such an extension of our theory seems of interest for an understanding of the modification, and eventually the disappearance, of the Weiss oscillations with increasing modulation strength.¹⁰ Moreover, it seems also inevitable for a consistent inclusion of the oscillatory contributions to the scattering conductivity considered by Vasilopoulos and Peeters.⁶

If the temperature is so low that the contributions

of individual Landau bands, or in future experiments even of individual subbands, to the thermodynamic DOS are resolved, the situation is expected to become even more interesting. Then screening effects become strongly magnetic field dependent,⁶⁴ and the treatment of the single-particle spectrum on the basis of a fixed superlattice potential may no longer be adequate. Instead, it may become necessary to base the transport theory on effective single-particle properties calculated from a self-consistently determined superlattice potential, which takes many-body effects into account.

At present, no direct experimental proof of the realization of a Hofstadter-type energy spectrum in the 2D ES's in GaAs/Al_xGa_{1-x}As heterostructures exists. However, we have shown that the characteristic subband splitting of the Landau levels predicted by the Hofstadter-type spectrum has specific consequences for the magnetotransport coefficients. Our theory, which takes these effects into account and exploits the consequences of this subband splitting, explains all the characteristic features of the Weiss oscillations observed in experiments on 2D ES's with weak 1D and 2D superlattice potentials. We are not aware of any alternative explanation of all these features. We therefore consider the existing experiments as a strong, although rather indirect, indication of the realization of the Hofstadter-type energy spectra. Thus we would like to encourage the preparation of high-mobility samples with lower electron density ($N_s < 10^{11} \text{ cm}^{-2}$) and smaller superlattice period ($a \sim 50 \text{ nm}$). In such samples a direct resolution of the subband splittings should become possible. This would open a decades-old playground of theorists to the band-structure tailoring nanostructure physics. Hopefully, an idea of the fragile beauty of Hofstadter's fractal butterfly will survive its birth into experimental reality.

ACKNOWLEDGMENTS

We gratefully acknowledge many stimulating, encouraging, and helpful discussions with Dieter Weiss, and also the fruitful cooperation of Ulrich Wulf, who performed the first numerical model calculations illustrating the mechanism for the suppression of the band conductivity.

APPENDIX A

In this appendix we sketch the derivation of the quasi-classical result for the band conductivity from the quantum-mechanical Kubo formula. According to Eqs. (24) and (33), the velocity matrix elements can be calculated from the $p \times p$ matrix,

$$\left[v_{\mu}^{(p)} \right]_{\kappa', \kappa} = \frac{-il^2}{\hbar} \sum_{\mathbf{g}} \bar{g}_{\mu} \tilde{V}_n(\mathbf{g}) \tilde{\delta}_{\kappa' - \kappa, [g_{\nu}/K_{\nu}]}^{(p)} \exp\{-il^2 [g_x k_y - g_y k_x + g_x (\kappa K_y + \frac{1}{2} g_y)]\}, \quad (\text{A1})$$

with $\bar{g}_x = -g_y$, $\bar{g}_y = g_x$, and $\tilde{V}_n(\mathbf{g}) = V_{\mathbf{g}} \mathcal{L}_n(\frac{1}{2} l^2 g^2)$.

This yields

$$\begin{aligned} \text{tr}^{(p)} \left[v_{\mu}^{(p)}(\mathbf{k}; n) \right]^2 &= \left(\frac{-i}{m\omega_c} \right)^2 \sum_{\mathbf{g}, \mathbf{g}'} \bar{g}_{\mu} \bar{g}'_{\mu} \tilde{V}_n(\mathbf{g}) \tilde{V}_n(\mathbf{g}') e^{-il^2[(g_x+g'_x)k_y - (g_y+g'_y)k_x + \frac{1}{2}(g_x g_y + g'_x g'_y)]} \\ &\quad \times \sum_{\kappa'=1}^p \sum_{\kappa=1}^p \delta_{[g'_y/K_y], \kappa' - \kappa}^{(p)} e^{-il^2 g'_x \kappa K_y} \delta_{[g_y/K_y], \kappa - \kappa'}^{(p)} e^{-il^2 g_x \kappa' K_y}. \end{aligned} \quad (\text{A2})$$

Since $[-n_y] = [p - [n_y]]$ and $\exp(-il^2 K_y g_y p) = 1$, the sum over κ' can be evaluated, and the last two sums in Eq. (A2) reduce to

$$\sum_{\kappa=1}^p e^{-il^2[(g'_x+g_x)\kappa K_y + g_x g'_y]} \delta_{[g'_y/K_y], [-g_y/K_y]}. \quad (\text{A3})$$

Next, one evaluates the k_y integral over the MBZ,

$$\begin{aligned} \sum_{\kappa=1}^p \int_0^{K_y} dk_y e^{-il^2(g'_x+g_x)(k_y + \kappa K_y)} \\ = \int_0^{pK_y} dk_y e^{il^2(g'_x+g_x)k_y} = pK_y \delta_{g'_x, -g_x}. \end{aligned} \quad (\text{A4})$$

From (A3) we know that $g'_y = g_y + tpK_y$, with an integer t . Then the k_x integral over the MBZ yields a $\delta_{t,0}$,

$$\int_0^{K_x/q} dk_x e^{il^2(g_y+g'_y)k_x} = \frac{2\pi}{qa_x} \delta_{g'_y, -g_y}. \quad (\text{A5})$$

Since $pK_x K_y/q = 2\pi/l^2$, one finally obtains

$$\int_{\text{MBZ}} d^2k \text{tr}^{(p)} \left[v_{\mu}^{(p)}(\mathbf{k}; n) \right]^2 = 2\pi \left(\frac{l}{\hbar} \right)^2 \sum_{\mathbf{g}} \bar{g}_{\mu}^2 |\tilde{V}_n(\mathbf{g})|^2. \quad (\text{A6})$$

The quasiclassical result (58) for the band conductivity follows immediately.

APPENDIX B

To evaluate Eq. (59) for $\hbar\omega_c \ll k_B T \ll E_F$, one replaces the sum over n with the integral over $E_n = \hbar\omega_c(n + \frac{1}{2})$, and uses the asymptotic expansion (9) to obtain

$$\Delta\sigma_{\mu\mu}^{\text{qcl}} = \frac{e^2 l^2}{\pi \hbar \Gamma_0} \sum_{\mathbf{g}} \bar{g}_{\mu}^2 |V_{\mathbf{g}}|^2 I_g \quad (\text{B1})$$

with

$$\begin{aligned} I_g &= \int_0^{\infty} \frac{dE}{\hbar\omega_c} \left[-\frac{df}{dE} \right] \frac{2}{\pi g R_c} \left[\frac{E_F}{E} \right]^{1/2} \\ &\quad \times \cos^2 \left(g R_c \sqrt{\frac{E}{E_F}} - \frac{\pi}{4} \right), \end{aligned} \quad (\text{B2})$$

where $E_F = \frac{1}{2} m \omega_c^2 R_c^2$. To leading order in the small parameter $2k_B T/E_F \ll 1$, one has

$$I_g = \int_{-\infty}^{\infty} dx \frac{\cos^2(g R_c - \frac{\pi}{4} + x g R_c k_B T/E_F)}{\pi \hbar \omega_c g R_c \cosh^2 x}. \quad (\text{B3})$$

Since

$$\int_{-\infty}^{\infty} dx \left[\frac{\cos(\alpha + \beta x)}{\cosh x} \right]^2 = 1 + \frac{\pi \beta \cos 2\alpha}{\sinh \pi \beta}, \quad (\text{B4})$$

one obtains Eq. (61).

¹D. Weiss, K.v. Klitzing, K. Ploog, and G. Weimann, Europhys. Lett. **8**, 179 (1989). See also *High Magnetic Fields in Semiconductor Physics II*, edited by G. Landwehr, Springer Series in Solid State Sciences Vol. 87 (Springer-Verlag, Berlin, 1989), p. 357.

²R.R. Gerhardtts, D. Weiss, and K.v. Klitzing, Phys. Rev. Lett. **62**, 1173 (1989).

³R.W. Winkler, J.P. Kotthaus, and K. Ploog, Phys. Rev. Lett. **62**, 1177 (1989).

⁴R.R. Gerhardtts, in *Science and Engineering of One- and Zero-Dimensional Semiconductors*, edited by S.P. Beaumont and C.M. Sotomayor Torres (Plenum, New York, 1990), p. 231.

⁵C.W.J. Beenakker, Phys. Rev. Lett. **62**, 2020 (1989).

⁶P. Vasilopoulos and F.M. Peeters, Phys. Rev. Lett. **63**, 2120 (1989); Surf. Sci. **229**, 96 (1990).

⁷R.R. Gerhardtts and C. Zhang, Phys. Rev. Lett. **64**, 1473 (1990); Surf. Sci. **229**, 92 (1990).

⁸C. Zhang and R.R. Gerhardtts, Phys. Rev. B **41**, 12 850 (1990).

⁹P. Středa and A.H. MacDonald, Phys. Rev. B **41**, 11 892 (1990).

¹⁰P.H. Beton, E.S. Alves, P.C. Main, L. Eaves, M. Dellow, M. Henini, O.H. Hughes, S.P. Beaumont, and C.D.W. Wilkinson, Phys. Rev. B **42**, 9229 (1990).

¹¹P.C. Main, P.H. Beton, E.S. Alves, N.W. Dellow, and M. Davison, Phys. Scr. **T39**, 169 (1991).

¹²R.R. Gerhardtts, Phys. Rev. B **45**, 3449 (1992).

¹³D. Weiss, C. Zhang, R.R. Gerhardtts, K.v. Klitzing, and G. Weimann, Phys. Rev. B **39**, 13 020 (1989).

¹⁴K. Ismail, T.P. Smith III, W.T. Masselink, and H.I. Smith, Appl. Phys. Lett. **55**, 2766 (1989).

¹⁵R.R. Gerhardtts, D. Pfannkuche, D. Weiss, and U. Wulf, in *High Magnetic Fields in Semiconductor Physics III*, edited by G. Landwehr, Springer Series in Solid State Sciences Vol. 101 (Springer-Verlag, Berlin, 1992), p. 359.

¹⁶D. Weiss, A. Menschig, K.v. Klitzing, and G. Weimann, Surf. Sci. **263**, 314 (1992).

¹⁷F.M. Peeters and P. Vasilopoulos, Phys. Rev. B **42**, 5899 (1990).

¹⁸H.L. Cui, V. Fessatidis, and N.J.M. Horing, Phys. Rev. Lett. **63**, 2598 (1989).

¹⁹D. Weiss, K.v. Klitzing, K. Ploog, and G. Weimann, Surf. Sci. **229**, 88 (1990).

- ²⁰R.R. Gerhardtts, D. Weiss, and U. Wulf, Phys. Rev. B **43**, 5192 (1991).
- ²¹E.S. Alves, P.H. Beton, M. Henini, L. Eaves, P.C. Main, O.H. Hughes, G.A. Toombs, S.P. Beaumont, and C.D.W. Wilkinson, J. Phys. Condens. Matter **1**, 8257 (1989).
- ²²H. Fang and P.J. Stiles, Phys. Rev. B **41**, 10171 (1990).
- ²³C.G. Smith, M. Pepper, R. Newbury, H. Ahmed, D.G. Hasko, D.C. Peacock, J.E.F. Frost, D.A. Ritchie, G.A.C. Jones, and G. Hill, J. Phys. Condens. Matter **2**, 3405 (1990).
- ²⁴D. Weiss, M.L. Roukes, A. Menschig, P. Grambow, K.v. Klitzing, and G. Weimann, Phys. Rev. Lett **66**, 2790 (1991).
- ²⁵P.G. Harper, Proc. Phys. Soc. London Sect. A **68**, 874 (1955).
- ²⁶M.Ya. Azbel', Zh. Eksp. Teor. Fiz. **46**, 929 (1964) [Sov. Phys. JETP **19**, 634 (1964)].
- ²⁷D. Langbein, Phys. Rev. **180**, 633 (1969).
- ²⁸A. Rauh, Phys. Status Solidi B **69**, K9 (1975).
- ²⁹R.D. Hofstadter, Phys. Rev. B **14**, 2239 (1976).
- ³⁰D.J. Thouless, in *The Quantum Hall Effect*, edited by R.E. Prange and S.M. Girvin, Graduate Texts in Contemporary Physics (Springer-Verlag, New York, 1987), p. 101.
- ³¹N.A. Usov, Zh. Eksp. Teor. Fiz. **94**, 305 (1988) [Sov. Phys. JETP **67**, 2565 (1988)].
- ³²G. Czycholl, Solid State Commun. **67**, 499 (1988).
- ³³R. Fleischmann, T. Geisel, and R. Ketzmerick, Phys. Rev. Lett. **68**, 1367 (1992).
- ³⁴D.J. Thouless, M. Kohmoto, M.P. Nightingale, and M. den Nijs, Phys. Rev. Lett. **49**, 405 (1982).
- ³⁵P. Středa, J. Phys. C **15**, L1299 (1982).
- ³⁶T. Ando, A.B. Fowler, and F. Stern, Rev. Mod. Phys. **54**, 437 (1982).
- ³⁷P. Středa, J. Kučera, and J. van de Konijnenberg, Phys. Scr. **T39**, 162 (1991).
- ³⁸C.T. Liu, K. Nakamura, D.C. Tsui, K. Ismail, D.A. Antoniadis, and H.I. Smith, Surf. Sci. **228**, 527 (1990).
- ³⁹F.M. Peeters and P. Vasilopoulos, in *Proceedings of the 20th International Conference on the Physics of Semiconductors*, edited by E.M. Anastassakis and J.D. Joannopoulos (World Scientific, Singapore, 1990), Vol. 2, p. 1589.
- ⁴⁰P. Vasilopoulos and F.M. Peeters, Phys. Scr. **T39**, 177 (1991).
- ⁴¹R.R. Gerhardtts, Phys. Scr. **T39**, 155 (1991).
- ⁴²The sample is considered as a part of an infinitely extended system. The plane waves are normalized on a length L_y , the ϕ_n on the total x axis. To count states correctly, x_0 is considered within a length L_x taken as a suitable (B -dependent) multiple of the period a . Finally, the limit $L_x, L_y \rightarrow \infty$ is taken.
- ⁴³M. Kohmoto, Ann. Phys. **160**, 343 (1985).
- ⁴⁴Alternative definitions of magnetic translations are used in the literature, e.g., $\exp(\frac{i}{\hbar}[\mathbf{R} \cdot \mathbf{p} + \frac{e}{c} \mathbf{A}(\mathbf{R}) \cdot \mathbf{r}])$ or $\mathcal{T}_{\mathbf{R}} \mathcal{E}_{\mathbf{R}}$, which differ from ours by a phase factor, according to the identity $\exp(P + Q) = \exp(P) \exp(Q) \exp(-\frac{1}{2}[P, Q])$, which holds if both operators P and Q commute with their commutator $[P, Q]$.
- ⁴⁵The result given in Ref. 40 for $V_x = V_y = V_0$, $V_{xy} = 0$, and half-integer values of the flux ratio ($p = 2$) is incorrect.
- ⁴⁶G.H. Wannier, Phys. Status Solidi **88**, 757 (1978).
- ⁴⁷A.H. MacDonald, Phys. Rev. B **28**, 6713 (1983).
- ⁴⁸T. Geisel, R. Ketzmerick, and G. Petschel, Phys. Rev. Lett. **66**, 1651 (1991).
- ⁴⁹F. Claro, Phys. Status Solidi B **104**, K31 (1981).
- ⁵⁰U. Sivan, Y. Imry, and C. Hartzstein, Phys. Rev. B **39**, 1242 (1989).
- ⁵¹G. Kirzenow, Surf. Sci. **263**, 330 (1992).
- ⁵²A.H. MacDonald, Phys. Rev. B **29**, 6563 (1984).
- ⁵³R. Gerhardtts and J. Hajdu, Z. Phys. **245**, 126 (1971).
- ⁵⁴R.R. Gerhardtts, Z. Phys. B **22**, 327 (1975).
- ⁵⁵R.R. Gerhardtts, Z. Phys. B **21**, 285 (1975).
- ⁵⁶For the illustrative purpose of the figures, we have approximated the spectral function (in the final analytical expressions) by a Gaussian, $A_{n,\alpha} = (2\pi\Gamma_0^2)^{-1/2} \exp[-(E - E_{n,\alpha})^2/2\Gamma_0^2]$, and not solved the self-consistency Eq. (38) numerically.
- ⁵⁷G. Czycholl and W. Ponischowski, Z. Phys. B **73**, 343 (1988).
- ⁵⁸R. Kubo, J. Phys. Soc. Jpn. **12**, 570 (1957).
- ⁵⁹P.H. Beton, P.C. Main, M. Davison, M. Dellow, R.P. Taylor, E.S. Alves, L. Eaves, S.P. Beaumont, and C.D.W. Wilkinson, Phys. Rev. B **42**, 9689 (1990).
- ⁶⁰In the captions of Fig. 4 of Refs. 20 and 15 the words "solid" and "dashed" should be interchanged.
- ⁶¹D. Weiss, in *Science and Engineering of One- and Zero-Dimensional Semiconductors*, edited by S.P. Beaumont and C.M. Sotomayor Torres (Plenum, New York, 1990), p. 221.
- ⁶²D.P. Xue and G. Xiao, Phys. Rev. B **45**, 5986 (1992).
- ⁶³Qian Niu, D.J. Thouless, and Yong-Shi Wu, Phys. Rev. B **31**, 3372 (1985).
- ⁶⁴U. Wulf, V. Gudmundsson, and R.R. Gerhardtts, Phys. Rev. B **38**, 4218 (1988).

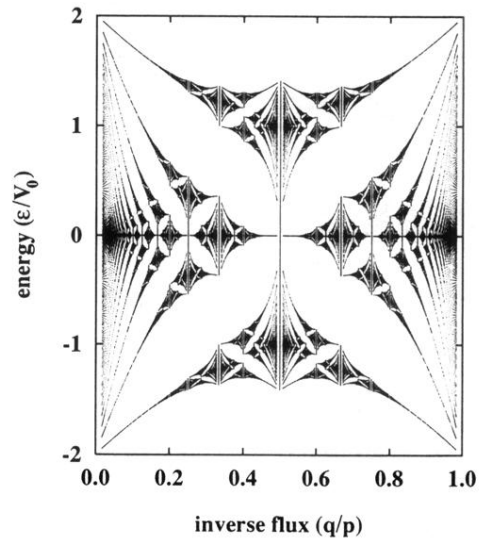


FIG. 2. Hofstadter's butterfly, showing the intervals of allowed values for the eigenvalue ϵ_α of Harper's Eq. (18), in units of $V_0 = V_x = V_y$, for rational values of the flux ratio $\Phi/\Phi_0 = p/q$, as a function of q/p .

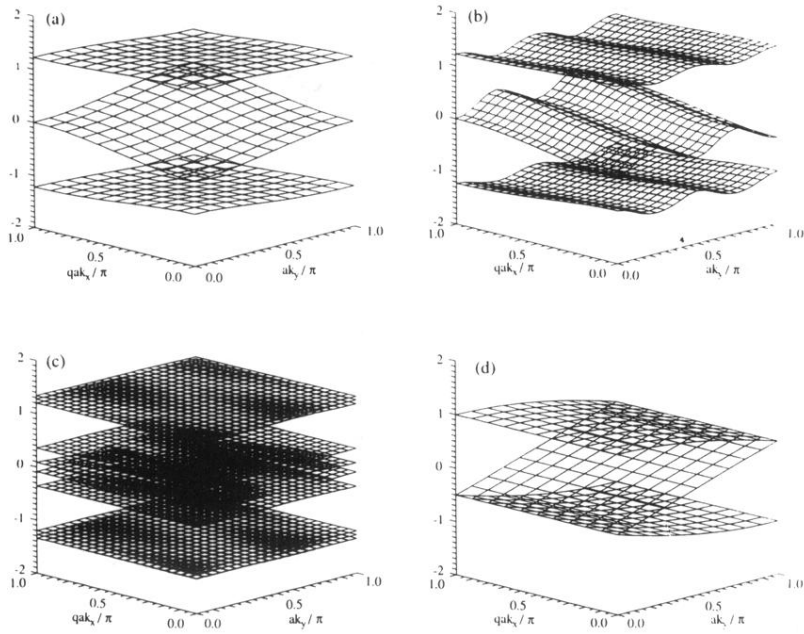


FIG. 3. Energy bands over one-quarter of the magnetic Brillouin zone. The scaled energy values $\varepsilon(\mathbf{k}, j)$ (without the Laguerre factors; see the text) are plotted in units of V_x , (a)–(c) for the Hofstadter case $V_y = V_x$ and for the values $p/q = 3/1$ (a), $3/4$ (b), $10/3$ (c) of the flux ratio, and (d) for a 1D superlattice ($V_y = 0$) and $p/q = 3/1$.

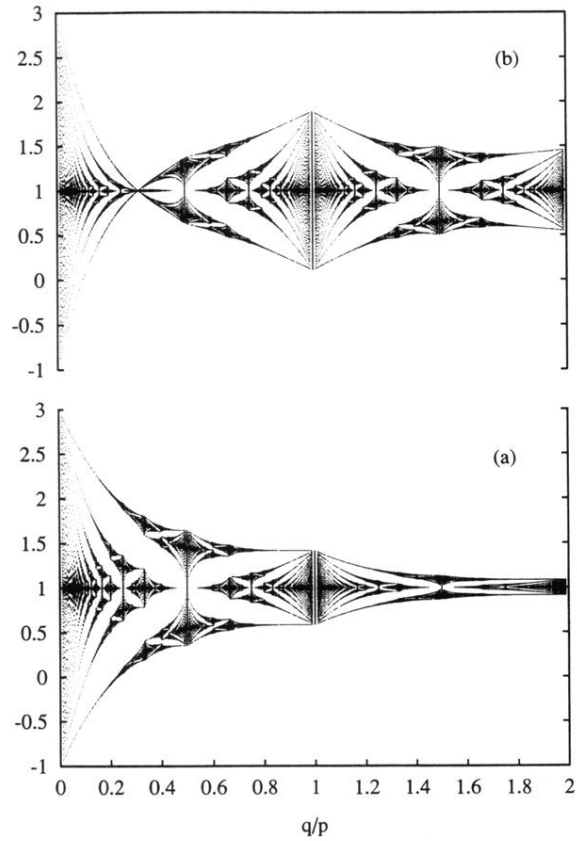


FIG. 4. Allowed values for the energy correction $\tilde{E}_{n,\alpha}$ (in units of V_0) to the n th Landau energy owing to the superlattice potential $V(x, y) = V_0[1 + \cos Kx + \cos Ky]$, versus rational values of the inverse flux ratio $l^2 K^2 / 2\pi \equiv \Phi_0 / \Phi = q/p$; (a) for $n = 0$, (b) for $n = 1$.

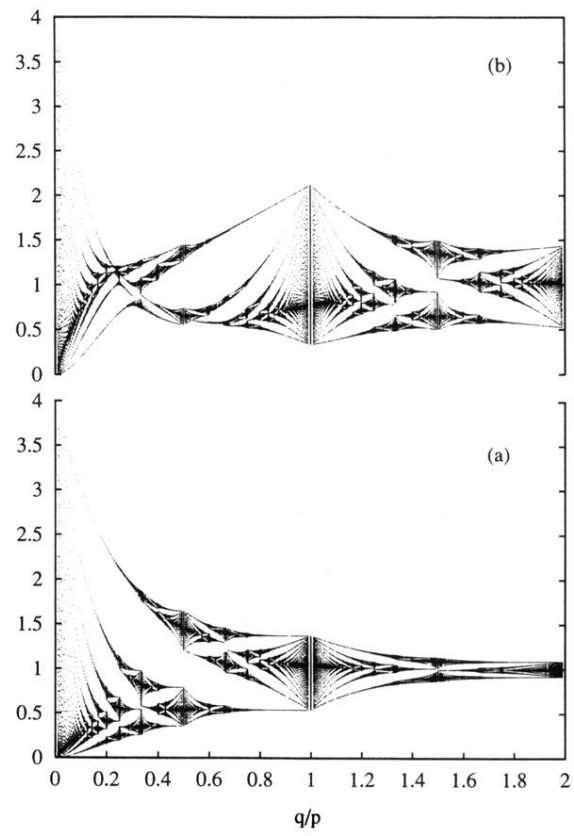


FIG. 5. The same as Fig. 4, but for the superlattice potential $V(x, y) = V_0(1 + \cos Kx)(1 + \cos Ky)$.